



UNIVERSITAT
POLITÈCNICA
DE VALÈNCIA



ESCUOLA TÉCNICA
SUPERIOR INGENIERÍA
INDUSTRIAL VALENCIA

Academic year:

Contents

ABSTRACT	3
RESUMEN	5
MEMORY	7
1. MOTIVATION AND AIM	9
1.1. Valorisation of agri-food residues	9
1.2. Objectives	11
2. INTRODUCTION	13
2.1. Biomass classification: origin and structure	13
2.1.1. Biomass origin	13
2.1.2. Biomass structure	15
2.2. Biomass as a source of energy	16
2.2.1. Energy generation strategies using biomass	17
2.2.2. Biomass as raw combustible	18
2.2.3. Biofuels from biomass	18
2.3. Valorisation of beer residues	19
2.3.1. Industrial process for beer production	20
2.3.2. Brewery by-products	22
2.2.3. Uses and possibilities for the brewer's spent grains	23
3. MATERIALS AND METHODS	25
3.1. Materials, beer production and sample preparation	25
3.1.1. Pilot-scale brewing process	25
3.1.2. Beer spent grain post-processing for characterisation	25
3.2. Proximate analysis	27
3.3. Ultimate analysis	28
3.4. Calorific value	28
3.5. Thermogravimetric analysis (TGA)	29
3.6. Kinetic analysis of the thermo-oxidative decomposition of biomass	30
3.6.1. Calculation of the activation energy	32
3.6.2. Analysis of the kinetic function	34

3.6.3. Analysis of the pre-exponential factor	35
3.7. Combustion of BSGs in a pilot incineration plant.....	36
4. RESULTS AND DISCUSSION	37
4.1. Biomass sample analysis	37
4.1.1. Proximate analysis.....	37
4.1.2. Ultimate analysis	38
4.1.2. Calorific value	39
4.2. Thermo-oxidative stability.....	39
4.2.1. Thermo-oxidative stability at a single heating rate.....	39
4.2.2. Thermo-oxidative stability as a function of the heating rate.....	41
4.3. Model-free kinetic analysis	46
4.3.1. Calculation of apparent activation energy	46
4.3.1.1. Single- α analysis	46
4.3.1.2. Multiple- α analysis for the global process	47
4.3.1.3. Multiple- α analysis for the decomposition in two main stages	51
4.3.2. Calculation of kinetic function and pre-exponential factor	58
4.4. Pelletised BSGs as combustion fuel.....	64
5. CONCLUSIONS	67
Bibliography.....	69
ECONOMIC STUDY.....	73
1. LABOUR COST	74
2. EQUIPMENT AND INSTRUMENTATION COST	74
3. FUNGIBLE MATERIAL COST.....	75
4. OTHER COSTS	76
5. FINAL COSTS	76

ABSTRACT

Nowadays, the accumulation of huge amounts of food wastes every year has led to environmental degradation and especially to significant loss of valuable material that could otherwise be exploited as new health-promoting ingredients, as additives, or in the production of bioenergy. Increasing efforts are being directed towards the reuse of agro-industrial by-products, from both an economic and environmental point of view.

A steady consumption of beer results in a steady output of residues. Brewer's spent grain (BSG) is the most abundant by-product generated in the beer-brewing process. It is a readily available by-product produced in large quantities throughout the year. BSG consists of the barley grain husks together with parts of the pericarp and seed coat layer that is obtained as solid residue after the production of beer wort. It is rich in fibres and proteins but, despite the wide range of possible applications, its main use is limited to animal feed or simply deposition to landfills. The study of alternative uses of BSG is appropriate, not only from the perspective of the brewer who can benefit from the valorisation of the produced by-product but also from an environmental outlook as the recycling and re-use of industrial wastes and by-products has become increasingly essential. However, a significant understanding gap regarding the variability of this low-cost residue, its influence in the valorisation process and its use in biorefineries exist.

This study attempts to characterize two different types of BSGs (ORISC and WHEAT) and the malts by which they are composed in terms of elemental composition, higher heating value, content of volatiles, fixed carbon, humidity, ash yield and to study the kinetic mechanism of decomposition during thermo-oxidative combustion. The two beers were produced starting from kits supplied by Spanish company Tu Cerveza Casera Homebrew. These are identified as "Old Rasputin Imperial Stout Clone" and "Wheat" kits. In terms of methodology, proximate analysis, ultimate analysis and calorific values were performed, as like as thermogravimetric analysis (TGA).

Valuable parameters were obtained by the application of Thermogravimetric Analysis (TGA). Thermogravimetric thermograms were determined at different heating rates, using oxygen as oxidative atmosphere. The thermo-chemical reactions were mathematically described through the definition of the main kinetic parameters: activation energy (E_a), pre-exponential factor (A), model of reaction ($f(\alpha)$). The so-called kinetic triplet was calculated through the application of iso-conversional methods, Master-Curves and Perez-Maqueda criterion.

The results of this study will serve as the baseline for the description of the energy recovery process in a reactor that uses brewer's spent grain residues as feedstock.



UNIVERSITAT
POLITÈCNICA
DE VALÈNCIA



ESCOLA TÈCNICA
SUPERIOR ENGINYERIA
INDUSTRIAL VALÈNCIA

RESUMEN

La acumulación de enormes cantidades de desechos alimentarios provoca cada año una gran degradación ambiental y, especialmente, una pérdida significativa de material valioso que de otro modo podría explotarse en otros ámbitos como materia prima en la industria de la alimentación o en la producción de bioenergía. De hecho, se están realizando esfuerzos cada vez más importantes encaminados a la reutilización de subproductos agroindustriales, tanto desde el punto de vista económico como medioambiental.

La industria cervecera, con una gran producción a nivel mundial, resulta en la generación de un flujo constante de residuos. El grano exhausto de la cerveza (BSG) es el subproducto más abundante generado en el proceso de elaboración de esta bebida. Es un subproducto fácilmente disponible y de bajo coste, que consiste en la cáscara del grano de cebada junto con partes del pericarpio y la capa de la cubierta de la semilla que se obtiene como residuo sólido después de la producción de mosto de cerveza. Aunque es una fuente rica en fibras y proteínas, su uso principal se limita a la alimentación animal o simplemente al depósito en vertederos, a pesar de la amplia gama de posibles aplicaciones que ofrece. El aprovechamiento de estos recursos alternativos basados en BSG permitiría beneficiar a la industria cervecera a través de la valorización de este y también desde una perspectiva medioambiental. Sin embargo, existe una falta de conocimiento con respecto a la variabilidad de este residuo de bajo coste, su influencia en los procesos de valorización y su uso en biorrefinerías.

Este estudio pretende caracterizar dos tipos diferentes de BSG, obtenidos durante la producción de cerveza en una planta piloto a partir de las mezclas ORISC y WHEAT, así como de las maltas que las componen. Se estudió la composición, el poder calorífico superior, el contenido de volátiles, el carbono fijo, la humedad y la generación de cenizas. Además, se realizó el estudio del mecanismo cinético de descomposición durante la degradación termo-oxidativa a través de análisis dinámicos en un analizador termogravimétrico (TGA) a distintas velocidades de calentamiento en atmósfera oxidativa.

Se obtuvieron valiosos parámetros a partir de los ensayos de estabilidad termo-oxidativa, y se describieron los modelos matemáticos para las reacciones de descomposición termoquímica mediante la evaluación de los principales parámetros cinéticos: energía de activación (E_a), factor pre-exponencial (A), modelo de reacción ($f(\alpha)$). El denominado triplete cinético se calculó mediante la aplicación de métodos isoconversionales, el uso de Curvas Maestras y la validación con el criterio de Pérez-Maqueda.

Los resultados de este estudio sirven como base para la descripción del proceso de recuperación de energía en un reactor, utilizando los residuos de granos gastados de la industria cervecera como materia prima como vector energético.



UNIVERSITAT
POLITÈCNICA
DE VALÈNCIA



ESCOLA TÈCNICA
SUPERIOR ENGINYERIA
INDUSTRIAL VALÈNCIA



UNIVERSITAT
POLITÈCNICA
DE VALÈNCIA



ESCOLA TÈCNICA
SUPERIOR ENGINYERIA
INDUSTRIAL VALÈNCIA

MEMORY



UNIVERSITAT
POLITÈCNICA
DE VALÈNCIA



ESCOLA TÈCNICA
SUPERIOR ENGINYERIA
INDUSTRIAL VALÈNCIA

1. MOTIVATION AND AIM

1.1. Valorisation of agri-food residues

Biomass can be generally defined as any hydrocarbon material source, including natural and derived structures, such as woody and herbaceous species, woody wastes (from forest thinning and harvesting, timber production and woodworking residues), agricultural and industrial residues, municipal solid waste, sawdust, grass, waste from food processing, animal wastes, aquatic plants and industrial and energy crops, as shown in **Figure 1.1**.

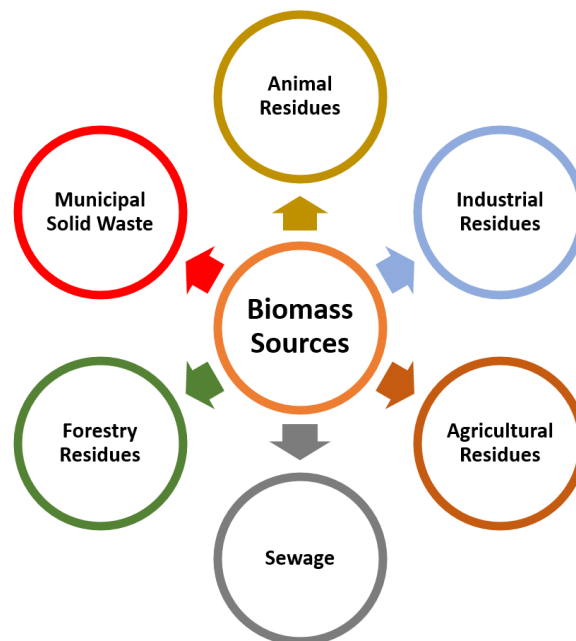


Figure 1.1. Biomass sources.

Among other uses of biomass, special interest is given to the production of energy. Dedicated crops are specifically produced for energy uses, these require relatively high photosynthetic efficiency, and possess high carbohydrate content and other hydrocarbon materials. However, most of the biomass energy is produced from wood and wood wastes (64%), followed by solid waste (24%), agricultural waste (6%), and landfill gases (6%).

There are several benefits of employing biomass for energy generation and biofuels production. Among them, it may be mentioned environmental, economic, social, and energy benefits. The use of biomass for the production of bioenergy can help to reduce greenhouse gases, contribute to the growth of healthier forests, enhance rural economies, and decrease the dependency on foreign oil.

The final use for biomasses influences the managing and practices to optimize the production system. A complete understanding of the chemical structure and of major components in biomasses is very important in the development of processes for producing derived fuels and chemicals. Biomass has a complex chemical composition, and both organic and inorganic constituents are important for the controlling and conversion processes. The leading compounds of plant biomasses are cellulose (C_6 polymers), hemicellulose (predominantly C_5 polymers but also C_6 species) and lignin. Biomass also

includes organic compounds like extractives, non-structural compounds mostly soluble in water and/or numerous organic solvents (fatty acids, lipids, terpenoids, phenolic compounds, glycosides, proteins, triglycerides, terpenes, waxes, cutin, suberin, flavonoids, betalains, alkaloids).

Biomass, and in particular food and agricultural residues, has emerged as a suitable feedstock for the new energy recovery processes due to its capacity in energy production, with High Heating Values (HHV) around 15-17 MJ/kg [1]. Their high production rates and the necessity to find them a better and suitable management have pointed them out as a feasible alternative to traditional fuels.

Brewery industry gives a huge contribution to biomass production. Beer is one of the oldest and most widely consumed alcoholic drinks in the world, and the third most popular drink overall after water and tea. Beer production industry generates four main solid wastes: the brewer's spent grain (derived from the grain processing), hot trub (protein coagulation that occurs during the boiling of the wort), residual brewer's yeast (microbial fermentative activity) and the diatomaceous earth (result of the beer clarification process). In terms of amount, considering the global production, almost 1.91 billion hectolitres in 2019 [2], it results in the generation of approximately 39 billion kg of brewer's spent grain (BSG) [3], 573 million kg of hot trub, and 3.82 billion kg of residual yeast. Even if the progress in technologies have permitted improvements in the process, in terms of quantity of by-products and in terms of efficiency, the quantity of these by-products, mostly spent grains, residual brewing yeast and trub is difficult to reduce.

Although deposition of these residues may be a reasonable option for management, from an economical perspective, new uses of this waste may be explored. By-products could undergo material or energy valorisation. They can be used as a renewable source for energy production but also, for the extraction of high-value components, such as proteins, polysaccharides, fibres, flavour compounds and phytochemicals.

The main components in the residues of beer production process are water, lignocellulosic compounds (hemicellulose, cellulose and lignin) and extractives. They present a great composition and morphological heterogeneity and thus, a study of their thermal properties becomes essential to understand the degradation mechanism of these solid-state reactions prior to its use as energy vectors.

According to literature, gasification is recognized as the best technique for thermo-chemical conversions of biomass [4]. Different reactor configurations could be used to perform these kinds of reactions, such as Fixed Bed Reactors, Fluidised Bed Reactors or Spouted Bed Reactors (SBR) among others [5]. However, if the aim is the implementation of a biomass in the industrial scale application, a deep understanding of the thermal behaviour of the biomass when submitted to high temperature heterogeneous reactions is necessary in order to find the best operational conditions in terms of design, scale-up and feasibility [6].

A useful method for the evaluation of parameters for the design and optimisation of the device can be obtained by means of the application of thermogravimetric analysis (TGA) when non-isothermal multiple heating rates are applied [7]. This methodology is necessary to model the combustion in an industrial scale process, to control the product yield and to correctly design it [8]–[10].

From these analyses, the main kinetic parameters can be calculated and serve as the baseline for the energy valorisation of beer spent grain in large-scale processes.

1.2. Objectives

The main objective of this work is to study the thermo-oxidation process of brewer's spent grain (BSG) residues of beer process production and the malts by which these are prepared to evaluate their suitability in the production of energy. This global purpose will be achieved by means of the following partial objectives:

- Determine the content in moisture, volatiles, fixed carbon and ash yield both for mashed malts and BSGs through proximate analysis.
- Determine the elemental composition of brewer's spent grains samples by means of ultimate analysis.
- Evaluate the calorific value of brewer's spent grain samples using Channiwala and Parikh relationship.
- Evaluate the peak temperatures and the minimum/maximum temperatures at which malts and BSGs decompose.
- Assess the behaviour and the reactions occurring during multiple heating rate thermogravimetric analyses under oxidative conditions.
- Estimate the minimum amount of energy to provide to the different components of BSGs and malts to start the decomposition reaction under oxidative atmosphere.
- Establish the decomposition mechanisms of reaction of the different components by the use of Master-Curves and Perez-Maqueda criterion.
- Validate the obtained results using a pilot incineration plant.



UNIVERSITAT
POLITÈCNICA
DE VALÈNCIA



ESCOLA TÈCNICA
SUPERIOR ENGINYERIA
INDUSTRIAL VALÈNCIA

2. INTRODUCTION

This chapter includes the definition of the biomass, a brief description of chemical characteristics and the potential applications of biomasses as a source to produce energy and valuable materials, as well as an overview of the main thermochemical process for biomass conversion. Since this study is focused on the characterisation and valorisation of beer residues from brewery industry, this chapter ends with a focus on the brewery residues and the options in the valorisation of this kind of biomass.

2.1. Biomass classification: origin and structure

2.1.1. Biomass origin

According to Oxford English Dictionary, the term “biomass” appeared first in the literature in 1934. Russian scientist Bogorov used the term biomass as nomenclature in the Journal of the Marine Biological Association. The weight of marine plankton (*Calanus finmarchicus*) after drying was measured and collected for investigating the seasonal growth change of plankton. This dried plankton was termed biomass [11].

In the EU Renewable Energy Directive, biomass is described as “the biodegradable fraction of products, waste and residues from agriculture (including vegetal and animal substances), forestry and related industries, as well as the biodegradable fraction of industrial and municipal waste. It includes all land and water-based vegetation, as well as all organic wastes. Biomass is derived from the reaction between carbon dioxide in the air, water and sunlight, via photosynthesis, to produce carbohydrates that form the building blocks of biomass” [12].

Biomass resources are sometimes termed biomass feedstocks. This name is used when they are available on a renewable basis and are used directly as a fuel or converted to another form or energy. Biomass feedstocks include dedicated energy crops, agricultural crop residues, forestry residues, algae, wood processing residues, municipal waste and wet waste. Wet waste includes crop wastes, forest residues, purpose-grown grasses, woody energy crops, algae, industrial wastes, sorted municipal solid waste (MSW), urban wood waste, and food waste. These biomass feedstocks are briefly described below.

Dedicated energy crops

Dedicated energy crops are non-food crops grown specifically for use as biomass feedstock that are cultivated on marginal land (land not dedicated to conventional crops like corn and soybeans). These are divided into two categories: herbaceous energy crops and woody energy crops. Herbaceous energy crops are perennial (plants that live for more than 2 years) that do not contain woody material. They are exemplified by grasses that are harvested annually after reaching full productivity (2 to 3 years). Examples include energy cane, switchgrass, miscanthus, sweet sorghum, tall fescue, kochia, wheatgrass. Short-rotation woody crops are fast-growing softwood and hardwood trees with short harvest rotation. They are harvested within 5 to 8 years of planting. These include hybrid poplar, hybrid willow, silver maple, eastern cottonwood, green ash, black walnut, sweetgum, and sycamore. They have longer harvest rotations than most herbaceous crops but compensate this by producing higher yields of biomass.

Agricultural crop residue

Agricultural crop residues can be divided in two categories: field and process residues. Field residues are those left in the field after harvesting and include stalks and stubble (stems), leaves, and seed pods. While process residues are those left after the processing of a crop into a useful resource, these category includes husks, seeds, malt bagasse, molasses and roots. Agricultural crops can be used as fertilizers, as animal fodder and soil amendment.

Forestry residues

Even forestry biomass feedstocks can be splatted into two categories: forest residues left after logging timber (including limbs, tops, and culled trees and tree components that would be otherwise unmerchantable) and whole-tree biomass harvested explicitly for biomass. These woody residues can be collected to be used in bioenergy production even if, habitat should maintain proper nutrient and hydrologic features.

Algae

Algae as feedstocks for bioenergy is referred to different groups of highly productive organisms as microalgae, macroalgae (seaweed), and cyanobacteria. Numerous algae make use of sunlight and nutrients to create biomass, which contains key components as lipids, proteins, and carbohydrates that can be converted and upgraded to a variety of biofuels and products. According to their strain, algae can grow in different environments: fresh, saline, or brackish water and in surface water sources, groundwater, or seawater.

Wood processing residues

Wood processing generates by-products and waste outputs that are called wood processing residues and normally carry out considerable energy potential. For example, wood treated to obtain products or pulp generates unexploited sawdust, bark, branches, and leaves/needles. These kinds of residues, instead of being discarded, could be converted into biofuels or useful bioproducts. Moreover, these are already collected at the point of processing thus, they could be convenient and reasonably cheap sources of biomass for energy production.

Sorted municipal waste

Sorted municipal waste category includes mixed commercial and residential garbage, such as yard trimmings, paper and paperboard, plastics, rubber, leather, textiles, and food wastes. MSW for bioenergy is both an opportunity to produce biomass energy but also to reduce the volume of residential and commercial waste in landfills.

Wet waste

Wet waste feedstocks include commercial, institutional, and residential food wastes (particularly those currently disposed in landfills). In particular, the category includes: biosolids rich in organic matter, manure slurries from concentrated livestock operations, organic wastes from industrial operations, and biogas, which is the gaseous product of the anaerobic digestion of organic matter and can be produced in anaerobic conditions and in a controlled environment from any of the above-mentioned

feedstock streams. Production of energy from these wet wastes can help create additional revenue for rural economies and solve waste-disposal problems.

2.1.2. Biomass structure

For a proper utilisation of biomass in the production of fuels, chemicals and energy, a deep knowledge on its chemical structure and main composition must be achieved. Biomasses have a complex chemical composition where both organic and inorganic components can be found, which play an important role in conversion processes. Plant-based biomasses are mainly composed of cellulose (C_6 polymers), hemicellulose (predominantly C_5 polymers but also C_6 species) and lignin. However, biomass can also involve lipids, proteins, simple sugars, starches, water, ash, and other compounds.

Cellulose is a linear crystalline polysaccharide, with general formula $(C_6H_{10}O_5)_n$. It works as framework substance between hemicellulose and lignin, making up 40-50% of wood, as represented in **Figure 2.1**. This polymer is formed from repeating units of cellobiose, a disaccharide of linked glucose moieties. Hemicellulose is a matrix substance between cellulose microfibrils. It is a polysaccharide of variable composition containing mainly five (including xylose and arabinose) but also six carbon monosaccharide units (including galactose, glucose, and mannose). Hemicelluloses constitute 20-30% of wood and other biomasses. Generally, it has higher concentrations in hardwoods than softwoods. The most abundant monomeric unit of hemicelluloses is xylan.

Lignin is a highly branched material, constituted mainly of cross-linked phenolic polymers. The structure varies among different plants. Softwood lignin is composed mainly of guaiacyl units stemming from the precursor trans-coniferyl alcohol. Hardwood lignin is composed mostly of guaiacyl and syringyl units derived from trans-coniferyl and trans-sinapyl alcohols. Grass lignin contains p-hydroxyphenyl units deriving from trans-p-coumaryl alcohol. Almost all plants contain all three guaiacyl, syringyl, and p-hydroxyphenyl units in lignin. The lignin contents on a dry basis generally range from 10% to 40% by weight in various herbaceous species [13].

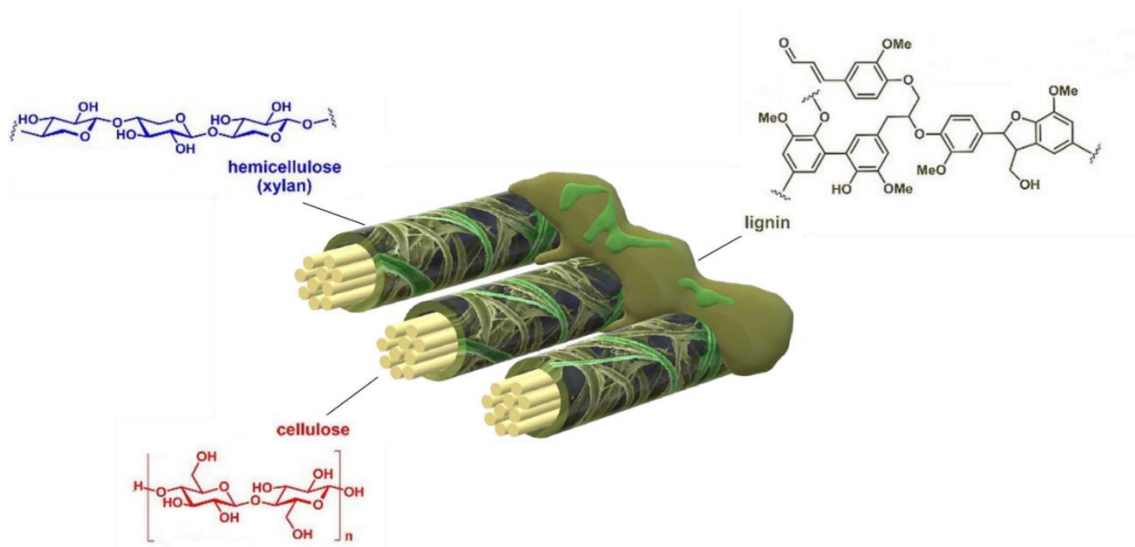


Figure 2.1. Basic components of lignocellulosic materials.

2.2. Biomass as a source of energy

Biomass can be used as a source of energy for production of electricity, heat, and in the production of gaseous and liquid fuels. After the sun, it is our oldest source of energy and is among the most valued and available resource on Earth. Biomass, as solar energy, is stored in chemical form in plants and animal materials and could be used as a renewable energy resource in solid, liquid, and gaseous form of energy sources. Global usage of bioenergy is estimated to rapidly increase, mainly to produce heat and power. In 2014 it was estimated that its use will become more than double in 2035 [14].

In the context of biomass energy, the definition of biomass refers to those crops, residues, and other biological materials that can be utilized as a substitute for fossil fuels in the production of energy and other products. In biomasses, the energy coming from sunlight is stored in chemical bonds. When the bonds between adjacent carbon, hydrogen, and oxygen molecules get broken by digestion, combustion, or decomposition, the chemical energy from these substances are released (biomass energy).

Biomass resources are expected to play an important role in meeting the upcoming energy needs. The approach in their use must be carefully examined in view of diverse cultural, socioeconomic, and technological factors in each geographical area. Agricultural and agro-industrial wastes can supply a cheaper source of energy and useful low sulphur fuel, which can be produced and stored.

The chemical composition of the biomass controls its energy density. The moisture level in biomass may vary from 10% to 60%, or even more in case of some organic wastes [15]. For this reason, raw biomass energy potential is low. This results in an increase in the transport costs and fuel cost per unit of energy produced. For reducing the transportation costs and so improve the conversion efficiency, the energy density of biomass feedstock should be upgraded by means of drying by using natural or accelerated processes. Other techniques comprise torrefaction, pelletizing or briquetting, and conversion to charcoal. Ash content is another critical issue concerning biomass feedstock. Ash generates deposits inside the combustion chamber and gasifier which is called “slagging” and “fouling”. These can weaken the performance of the conversion process and raise the maintenance costs. Higher amount of ash is present in grasses, bark, and agricultural crop residues. In woody residues, ash content is normally lower.

Renewable energy systems are rapidly becoming more efficient and cheaper and their share of total energy consumption is increasing. In 2018, more than two-thirds of worldwide newly installed electricity capacity was renewable [16]. Renewable energy markets are expected to continue to grow rapidly in next decades. Nowadays, at least two countries, Iceland and Norway, are already able to generate all their electricity utilizing renewable, and many other countries have the set a goal to reach 100% renewable energy in the next future. At least 47 nations around the world already have over 50% of electricity from renewable resources [17]. Renewable energy resources exist over wide geographical areas, in contrast to fossil fuels, which are concentrated in a limited number of countries. Rapid implementation of renewable energy and energy efficiency technologies is resulting in significant energy security, climate change mitigation, and economic benefits.

European Commission has expanded the assistance to programs in the fields of energy efficiency and renewable energy sources. The actual trend is focused on the support of research, together with other regulatory and economy-based actions, to effectively increase the share of renewable energies. It is

proved that bioenergy has the highest contribution among renewable materials. Nowadays bioenergy is identified as the renewable resource that will make the most significant contribution for sustainable energy in the near to medium term. This is actually the only renewable resource that can directly replace fossil fuel-based energy [18].

However, the current use of renewable sources for energy production is significantly lower than the one that could be. This is mostly due to quite high costs of the technologies of upgrading. In fact, the investment costs can be significantly higher related to fossil-fired plants [19]. This is due to the lower energy densities, the variety of characteristics and the objective to achieve a clean combustion that all together bring to larger plant size and higher efforts in conversion and clean-up technology. In particular, the lower energy density of biomasses with respect to fossil fuels, also brings to a higher effort required for transportation and storage of biofuels.

2.2.1. Energy generation strategies using biomass

There are three main methods of using biomass for the energy generation: burning it to produce heat and electricity; convert it into gaseous fuels such as methane, hydrogen, and carbon monoxide; and converting it to a liquid fuel. The liquid fuels are also termed biofuels.

For the conversion of biomass, thermochemical, biochemical and physicochemical approaches are usually considered. Actually, combinations of two or more of these routes may be used. Thermochemical conversion involves combustion, thermal gasification, and pyrolysis as well as several alternatives involving microwave, plasma arc, supercritical fluid, and other processing techniques. Products include heat, fuel gases, liquids, and solids. Biochemical and physicochemical processes are usually more intended to upgrade biomass components and produce products with higher economical value. Thermochemical routes can also be used in this case, as in the indirect production of methanol via gasification. The conversion approaches are integrally linked to the properties of the biomass. In many cases, the properties of the biomass used for its valorisation have not been properly characterized before to commercial implementation of a technology.

There are various factors which influence the choice of the conversion process. In general, these factors are the type of biomass, the quantity of biomass, the desired form of the energy, the end-use requirements, the environmental standards, the economic conditions and the project specific factors.

Usually, it is the form in which the energy is required which establishes the process route, followed by the types of biomass available and the biomass quantities. Conversion of biomass to energy is performed using these main following technologies. Each one is suitable for specific types of biomasses and results in specific energy products [20], [21]:

1. Thermal conversion: Heat is used with or without oxygen for converting biomass into energy. These technologies include direct combustion, pyrolysis, and torrefaction.
2. Thermochemical conversion: Heat and chemical processes are used in the production of energy from biomass. Gasification is a major process.
3. Biochemical conversion: Enzymes, bacteria, or other microbes are used for converting biomass into liquid fuels. It includes anaerobic digestion, and fermentation.

Conversion of biomass into useful products depends on the biomass properties, the requirement of the product and its applications. For woody biomass, the most frequent application is the thermochemical conversion route (combustion) to produce heat.

Gasification is the thermochemical conversion of biomass into combustible fuel in the presence of oxidant (lower than the stoichiometric combustion) conducted in a reactor called gasifier. Solid biomass can be converted into different liquid or gaseous fuels which may be further synthesized for various applications, including heating, cooking, power generation, and transportation. Different types of fuels and chemicals can be generated from product gases which can be used to replace petroleum-based chemicals. The main drawbacks in the valorisation are the higher cost associated with cleaning of the product gas from tar and unwanted contaminants such as alkali compounds; inefficiency because of the need of elevated temperatures; and the untested use of products as transportation fuels.

2.2.2. Biomass as raw combustible

Nowadays, the main types of biomasses used as combustible are wood, agricultural residues or solid waste residues. The main advantage in the use of biomass as combustible is its renewable nature, which does not promote neat carbon dioxide (CO₂) emission. The biomass energy can be obtained by burning biomass as if it was a fossil fuel. However, contrary to fossil fuel, when biomass is burned it release all the carbon dioxide which was absorbed by plant during growing. Thus, in this case the CO₂ is returning back to the atmosphere during its burning for the production of energy, while the CO₂ produced from fossil fuels is only going to atmosphere, where it increases the Earth's greenhouse effect and contributes to global warming.

The huge release of carbon is well-known to contribute significantly to climate change. Bioenergy can take care of this as it is a natural part of the carbon cycle in contrast to fossil fuel sources like oil, natural gas, and coal. Raw biomass energy sources are abundantly available everywhere, this means that problem of scarcity will never be encountered, while this is happening with fossil-based resources of fuel. Biomass is sustainable and does not exhaust future resources, this helps to reduce our actual state of overreliance on fossil fuel.

Useful bioenergy can be produced from waste generated from wood, forest residues, agricultural residues for producing heat and electricity, and, at the same time can resolve the waste disposal problems. Bioenergy production uses any type of waste that would have otherwise discarded into landfills. This also reduces the effect of waste in landfills to the environment.

Burning biomass trash turns waste into a usable form of energy. One ton of garbage contains about as much heat energy as 500 pounds of coal [22]. Garbage is not all biomass; perhaps half of its energy content comes from plastics, which are made by petroleum and natural gas. Power plants that burn garbage for producing energy are called waste-to-energy plants. These plants generate electricity as like as coal fired plants, but, the combustible in this case is garbage instead of coal.

2.2.3. Biofuels from biomass

Among the uses of biomass, it may be underlined the generation of landfill gas and biogas, and alcohol fuels such as ethanol or biodiesel.

Bacteria and fungi are able to eat dead plants and animals, causing them to rot or decay. A fungus on a rotting log is converting cellulose to sugars in order to feed itself. Although this process is quite slow in a landfill. Under anaerobic digestion conditions, methane gas is produced as the waste decays. Methane gas is colourless and odourless, but it is not harmless. The gas can cause explosions if it seeps into nearby homes and is ignited. New regulations require landfills to collect methane gas for safety and environmental reasons [23]. Landfills can collect methane gas, purify it, and use it as fuel. Methane can also be produced using energy from agricultural and human wastes. Biogas digesters are airtight containers or pits lined with steel or bricks. Waste put into the containers is fermented without oxygen to produce a methane-rich gas. This gas can be used to produce electricity, for cooking and lighting.

Ethanol is an alcohol fuel (ethyl alcohol) produced by fermenting the sugars and starches found in plants and then distilling them. Basically, any organic material containing cellulose, starch, or sugar can be converted into ethanol. Most of the ethanol produced in the United States comes from corn [24]. New technologies are producing ethanol from cellulose in woody fibres from trees, grasses, and crop residues.

Biodiesel is a fuel produced by chemically reacting alcohol with vegetable oils, animal fats, or greases, such as recycled restaurant fat, via a transesterification reaction. Most biodiesel today is made from soybean oil. Biodiesel is most often blended with petroleum diesel in ratios of 2% (B2), 5% (B5), or 20% (B20). It can also be used as “pure” biodiesel (B100). Biodiesel fuels are compatible with existing engines and can be used in actual diesel engines. Biodiesel does not contain sulphur, so it can reduce sulphur levels emissions. While removing sulphur from petroleum-based diesel results in poor lubrication, biodiesel is a better lubricant and can reduce the friction of diesel fuel in blends of only 1-2 percent. The disadvantage of biodiesel is that it has lower energy content with respect to fossil-based fuel.

2.3. Valorisation of beer residues

Brewery industry gives a huge contribution to biomass production. Beer is the most consumed alcoholic beverage in the world. The brewing industries produce millions of tons of residues, which represent a management issue from both ecological and economical point of view.

The valorisation of brewing by-products can be achieved either from a material or energy perspective. Material valorisation involves the extraction of high-value components such as proteins, polysaccharides, fibres, flavour compounds and phytochemicals, which can be reused as nutritionally and pharmacologically functional ingredients.

During the industrial beer production, four main solid wastes are generated: (i) the brewer’s spent grain derived from the grain processing; (ii) hot trub, as protein coagulation that occurs during the boiling of the wort; (iii) residual brewer’s yeast from microbial fermentative activity; and (iv) the diatomaceous earth because of the beer clarification process.

It is estimated that for every 100 litres of beer produced, 14 to 20 kg of brewer’s spent grain, 0.2-0.4 kg of hot trub, and 1.5-3 kg of residual brewer’s yeast are generated [25]. Considering the global production of beer, almost 1.91 billion hectolitres (in 2019) per year [2], the number of residuals result in the generation of approximately 30 billion kg of brewer’s spent grain (BSG), 573 million kg of hot trub, and 3.82 billion kg of residual yeas.

Nowadays the advantages in technologies made in the last twenty years have permitted the brewing industry huge savings in terms of process by-products. However, the quantity of certain by-products (spent grains, residual brewing yeast and trub) is difficult to reduce and their amount remains considerable.

2.3.1. Industrial process for beer production

The basic ingredients of beer production are water, malted barley, hops, and yeast. During production, beer goes through three main chemical and biochemical reactions: mashing, boiling and fermentation. In the mashing stage, malt starch is converted to fermentable sugars (mainly maltose and maltotriose) and non-fermentable sugars (dextrins), and proteins are partially degraded to polypeptides and amino acids. This enzymatic conversion stage produces sweet liquid called wort and a residual solid fraction called spent grains. After filtration, the wort is transferred to the brewing kettle where it is boiled with the addition of hops. During this process, the bitter and aromatic hop components will give typical beer qualities, such as bitter taste, flavour and foam stability. When the boiling ends, the liquid extract is separated from the spent hops to be further processed. A fraction of the hop components ends up in the trub (a precipitation product of the wort boiling process that may include insoluble hop materials, condensation products of hop polyphenols and wort proteins, and isomerised hop acids). During fermentation, the yeast cells will convert the fermentable sugars to ethanol and carbon dioxide. At the end of this stage, most of the cells are collected as spent yeast. **Figure 2.2.** schematizes the industrial brewery process and the by-products involved in the steps while **Table 2.1.** briefly describes each step in the process.

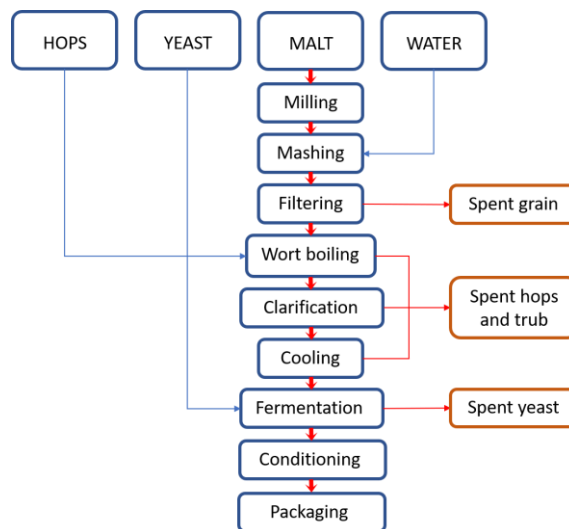


Figure 2.2. Schematic representation of an industrial brewery process and the by-products involved.

Table 2.1. Main stages during the industrial process for beer production.

<i>Malting</i>	Malting is the artificially induced germination of a crop to control the dissolution of grain. At this step barley grains are cleaned and then soaked in water for about 2 days. Then excess water is drained away and the barley are incubated for 4-5 days to allow germination, that allows the formation of highly active α -amylase, β -amylase and proteases enzymes as well as flavour and colour components.
----------------	---

<i>Kilning</i>	The germinated seed are then killed by slow heating at 80 °C during kilning. The kilning temperature must not harm amylase enzyme. Kilning temperature affects darkness of beer; higher temperatures imply darker beer produced.
<i>Milling</i>	At this step, dried barley grains are crushed between rollers to produced coarse powder called grist. Milling increases reactive surfaces for enzymes, in this way malt ingredients are easier to dissolve. Grain husk should be saved because it serves as filtration layer during lautering. The quality of milling has an impact on mashing and lautering and thus on quality of the resulting beer.
<i>Mashing</i>	Grist is mixed with water during mashing. Enzymes dissolve malt substances. Processes are regulated by temperature, residence time, pH-value, and water grist ratio. The resulting product is maintained at 65 °C for about 1 h. In these conditions, starch is hydrolysed by amylase enzyme to single sugar, maltose or dextrose. Similarly, protein is hydrolysed by proteolytic enzymes into small fragments and amino acids. The enzymatic hydrolysis strongly depends on pH and temperature.
<i>Lautering</i>	The aim of lautering is the separation of liquids (wort) and solids (spent grains). Husks act as a filter during this process. At first, liquid drains off. Then, residual spent grain is flushed several times with hot water. Increasing the temperature decreases the viscosity and separation is accelerated. The liquid obtained at this step is called beer wort.
<i>Wort boiling</i>	After lautering, wort is transferred to a boiling device (kettle) for 2-3 h and hop flowers are added at various intervals during boiling. Hops are dried female flower of hop plant <i>Humulus lupulus</i> . The quantity of hop flower used depends on the type of beer produced. Wort of boiling is important for the extraction of hop flavour to provide the pungent and aromatic character, to coagulate remaining protein, to inactivate enzymes that were active during mashing (otherwise causes caramelization of sugar), to sterilize and concentrate the wort. Moreover, hop contains α -resin and β -resin which gives bitter flavour as well as preservative action against gram positive bacteria and also contains pectin which is responsible for foam characteristic of beer.
<i>Fermentation, maturation and storage</i>	Beer industry uses strains of <i>S. carlsbergens</i> and <i>S. varum</i> which are bottom yeast and <i>S. cerevisiae</i> which is a top yeast. Yeast cells for inoculation are usually recovered from prior fermentation tank by treatment with phosphoric acid, tartaric acid or ammonium persulphate to reduce the pH and remove considerable bacterial contamination. Fermentation is usually carried out at 3-4 °C but it may range from 3-14 °C. Fermentation usually completes in 14 days. During fermentation yeast converts sugar mainly into ethanol and CO ₂ plus some amount of glycerol and acetic acid. For fermentation closed fermenter tank is preferred, so that CO ₂ liberated during fermentation can be collected for later carbonation step. The young green beer is stored at 0 °C for several weeks. During this period, precipitation of protein, yeast, resin and other unwanted substances take place and beer become clear. Ester and other compounds are also produced during ageing which gives taste and aroma. After ageing, the beer is carbonated by CO ₂ of 0.45-0.52%. Then it is cooled, clarified, filtered and packed in bottles, barrels and cans.
<i>Filtration and stabilization</i>	Often storage alone is not sufficient to guarantee immaculate taste and a clear or sparkling beverage. Artificial clarification takes place by filtration, centrifugation or adsorption. Grade of filtration and intensity of stabilization depend on market demands. In case of centrifugation colloids remain in beer, in filtration colloids and spoiling bacteria are retained according to pore size and in absorption clarification is based on affinity of substances to filter material. Finally, the filling process has the aim to conserve beer quality and to give an attractive appearance for consumers. It is the most expensive step, in terms of cost and

labour. Parameters like oxygen concentration in beer, partial pressure of CO₂ and cleaning/disinfection of inhibits contamination, are monitored. In particular, filling under pressure must be applied to retain dissolved CO₂. Moreover, air contact must be avoided to retain colloidal stability and flavour ($C_{O_2} \leq 0.01$ mg O₂/L).

2.3.2. Brewery by-products

Brewer's spent grain (BSG), hot trub, and residual yeast are called brewery solid or wet brewery wastes. They have high water content, but also high content of organic matter and are rich in carbohydrates, proteins, amino acids, minerals, vitamins and phenolic compounds. Their final disposal in the environment is difficult, suggesting their use for applications in industrial bioprocesses [25].

These main residues are responsible for the loss of approximately 20 %v of the water used in the brewing process [25], particularly due to their high-water content, usually between 80-90% [25]. This brings to high drag of wort and so retain of extracts, as well as of beer, leading to significant amounts of effluent formation. A fourth brewery residue may be also mentioned: diatomaceous earth, used in the filtration of final product to improve its brightness. Even if this residue can be avoided using another filter media, for economic reasons, in large scale breweries and countries where it is a habit of consumption of clear beer, this filter element is the most used. These by-products generated in the process have a high content of organic substances and so, a wide range of possible applications.

The brewer's spent grain, or malt bagasse, is the first and major solid by-product generated during the process, after mashing and filtration stage. This residue has a high nutritional value. From the process results a great volume of residue produced, with low or no cost to its acquisition. This residue corresponds to about 85% of the total waste generated in the brewing process [26].

This insoluble material consists of the barley grain husk in the greatest proportion and a remaining fraction not converted into fermentable sugars by the mashing process, mainly composed of pericarp and fragments of endosperm.

During the mashing step, milled malted grains are exhausted in order to extract all the important soluble compounds which constitute the sweet wort. In this step the BSG formed has an essential function as a filter element. During the mashing process, about 80% of the malt mass is solubilized, remaining in the bagasse the insoluble fractions.

After mashing and clarification, the wort is sent to the boiling stage, in which hop addition and extraction of its aroma and bitterness compounds take place (isomerization). At this stage, many mechanisms are involved; destruction of enzymes, colloidal stabilization, sterilization, dimethyl sulphide (DMS) and ketone compounds volatilization, development of colour, flavour and aroma compounds, calcium phosphate precipitation with reduction of pH, concentration and adjusting the initial extract. Until this point, the wort has high nitrogen content but here, it loses part of this component (about 6%) due to the formation of a precipitate called hot trub. Hot trub precipitate results predominantly from insoluble coagulation of high molecular weight proteins.

Then, during fermentation stage, brewing yeast tends to multiply 3-5 times in the reactor, particularly during the early hours, when oxygen is supplied to the wort. Fermentation stage is followed by a

resting period at low temperatures (maturation) when precipitation of the yeast mass and other fogginess compounds occurs. In brewing industry is common to reuse cell mass produced for the inoculation of new fermentation tanks, in general, as long as it does not compromise the sensory quality of the beverage. Once the mass cannot be reused, cells are removed from the process, generating new solid waste, called residual brewing yeast. Normally, this by-product is the second in terms of volume. The quantity of residual microbial biomass produced varies depending on the fermentation parameters (mainly aeration, temperature, and pH), type of microorganism (*Saccharomyces uvarum* or *Saccharomyces cerevisiae* usually), inoculum concentration and composition of brewer wort.

After fermentation and maturation there may still be considerable turbidity and chemical changes in the beer flavour that could take to alterations during periods of transport and storage. Deposition of yeast and haze components is a slow process, and normally not all medium turbidity is removed. Industrially, a further step of filtration is implemented. Nowadays the filter element most used is the diatomaceous earth. Diatomaceous earth is a material rich in silicates from fossils of prehistoric algae (diatomite) and today represents the most effective and used filtration method in brewing industry. Due to the retention of organic material, especially yeast, proteins and polyphenols, by the end of the filtration, cake mass can be increased three times or more, and this material cannot be used in subsequent filtration after its saturation. Thus, another solid residue is generated.

2.2.3. Uses and possibilities for the brewer's spent grains

As said, BSG is the major by-product in beer production, resulting every year in the production of million tons of this. In general, BSG composition varies with the species of barley, the malting process, the milling of malt, mashing and clarification. Exhausted malt are predominantly fibrous materials with significant protein content, containing nutritional value equivalent to about one fifth of the value of barley [25] [27]. The content of proteins can be between 15 to 26% and the content of fibres about 70%, those which can be divided in three fractions: cellulose (between 15.5 and 25%), hemicelluloses (mainly arabinoxylans, 28 to 35%) and lignin (approximately 28%). It may also contain lipids (between 3.9 and 10%), ash (2.5 to 4.5%), vitamins, amino acids and phenolic compounds [25].

Due to the high valuable composition, it can be investigated the use of this by-product in different applications. Many applications can be cited, such as animal and human nutrition, energy production by direct burning or for biogas production by anaerobic fermentation; charcoal production; adsorbent material in chemical treatments; cultivation of micro-organisms and obtaining bioproducts by fermentation; support for cell immobilization, among others.

In the work "Valorisation of raw brewers' spent grain through the production of volatile fatty acids" [28] raw BSG was used as feedstock in anaerobic digestion with the aim of producing VFA, which has a large potential in the production of bioplastics.

BSG is also be tested in fermentation to investigate the value addition of this process on the by-product [29]. In this cited work, it was proved that metabolites variations during fermentation provide enhanced nutrient content to BSG.

A material valorisation intended by Petr Klímek with the utilization of brewer's spent grain in the wood-based particleboard manufacturing consists in the substitution of wood particles with BSG particles

[30]. Unfortunately, in this case an increase in percentage of BSG particles used causes worsening in mechanical properties.

Many other works can be cited, mostly about the use of this by-product as animal dietary ingredient, while its application to human consumption is limited due to factors like the presence of bitter compounds, the difficulty to digest the thick cell wall and the high RNA content that cause increase in the level of uric acid in the blood and human tissues [25].

The large amounts of BSG make it the most studied and interesting by-product of the process even if hot trub and residual brewery yeast have huge range of applications, too. Nowadays, their main application is in the preparation of animal feed mixed with the brewer's spent grains.

Though, high porosity of diatomaceous earth residue makes it impossible to reuse and very difficult to dispose. The high quantity of organic material makes mandatory the calcination for the removal of those impurities. When treated in this way, it may be used to recover silicates for construction applications [31].

3. MATERIALS AND METHODS

In this chapter, an overview of the materials and experimental procedures for the preparation and characterization analyses is given.

3.1. Materials, beer production and sample preparation

In this study two different brewer's spent grains were used, after 20 L beer productions with the kits provided by the company *Tu Cerveza Casera Homebrew*. The kits are identified as "Old Rasputin Imperial Stout clone" (ORISC) and "Wheat" (WHEAT). Both beers were produced in a pilot-scale brewing installation, following the procedure provided by vendor. Moreover, according to the composition of these kits, malts composing the two kits were also purchased from the same company for comparison purposes. In particular, Carafa, Aroma, Pale Ale, CaraCrystal, Trigo and Pilsner (Pilsener) varieties were considered. **Table 3.1** gathers the different malt components for the analysed kits.

Table 3.1. Malt components of the analysed kits.

ORISC	WHEAT
<ul style="list-style-type: none">• Carafa• Aroma• Pale Ale• Crystal	<ul style="list-style-type: none">• Crystal• Trigo• Pilsener

3.1.1. Pilot-scale brewing process

Firstly, the malt mix was crushed in a malt mill. Crushing has to be not fine, it just has to break the grain without breaking the seeds chaff, which must remain intact. It is important for the filtering that will take place after the mashing process. Then the boiler was filled with water to make the malt mass. Then, the mashed malt was added and everything was mixed very well, so that every malt was in contact with water. At the end of this first step the malt mass was obtained.

Maceration is the saccharification of the starch. The malt grain contains starch, which was converted into simple sugars. Those sugars are necessary for subsequent fermentation. At this step the temperature was 67 °C during 1 h. Then, the mixture was heated up to 75 °C for 5 min, prior to filtering and rinsing. For fermentation, the obtained sugary solution is needed. The solid components of the solution after filtering are discarded, known as brewer's spent grain (BSG). Filtration was carried out through a perforated filter plate and gently rinsed with water at 78 °C. The remaining fraction in the filter (BSG) was dried weight and stored for further analyses.

3.1.2. Beer spent grain post-processing for characterisation

BSG obtained from previous step was removed from the filter and dried at 50 °C during 72 h. After that, humidity was low enough for the BSGs grinding. This procedure was carried out using a Moulinex Super Junior "S" grinder. The powders obtained were stored in a desiccator.

The same procedure was followed for the above-mentioned malts. Malts were treated according to the described procedure for the beer kits, involving the mash, maceration, filtering, rinsing, drying and grinding steps.

The appearance of the BSGs and malts before and after grinding as like as the microscopic images of dried powders is shown in **Table 3.2.** and **Table 3.3.** respectively. These powders, with a more homogeneous structure than grains, were used for all the analyses of this study.

Table 3.2. Macroscopic appearance of the milled and grinded brewer’s spent grains and microscopic images of the obtained powders. Scale bar represents 1 mm.

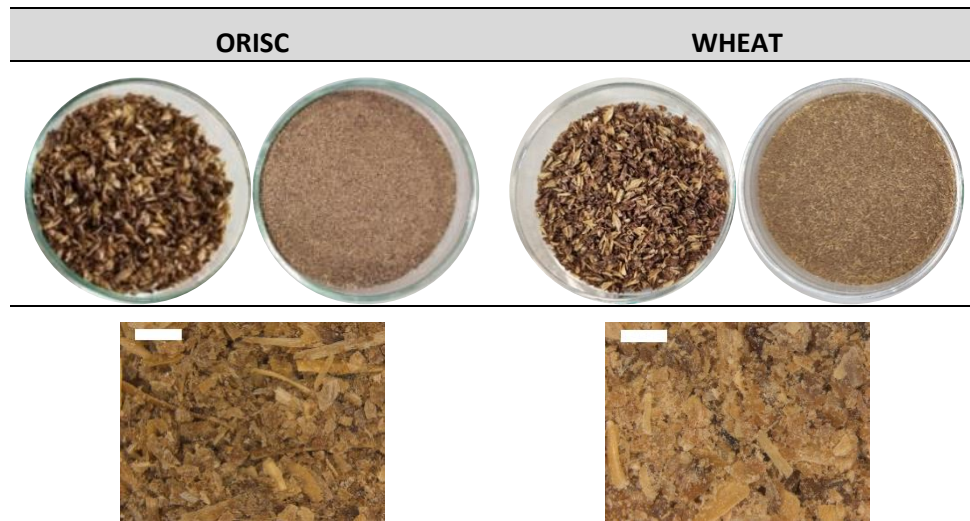
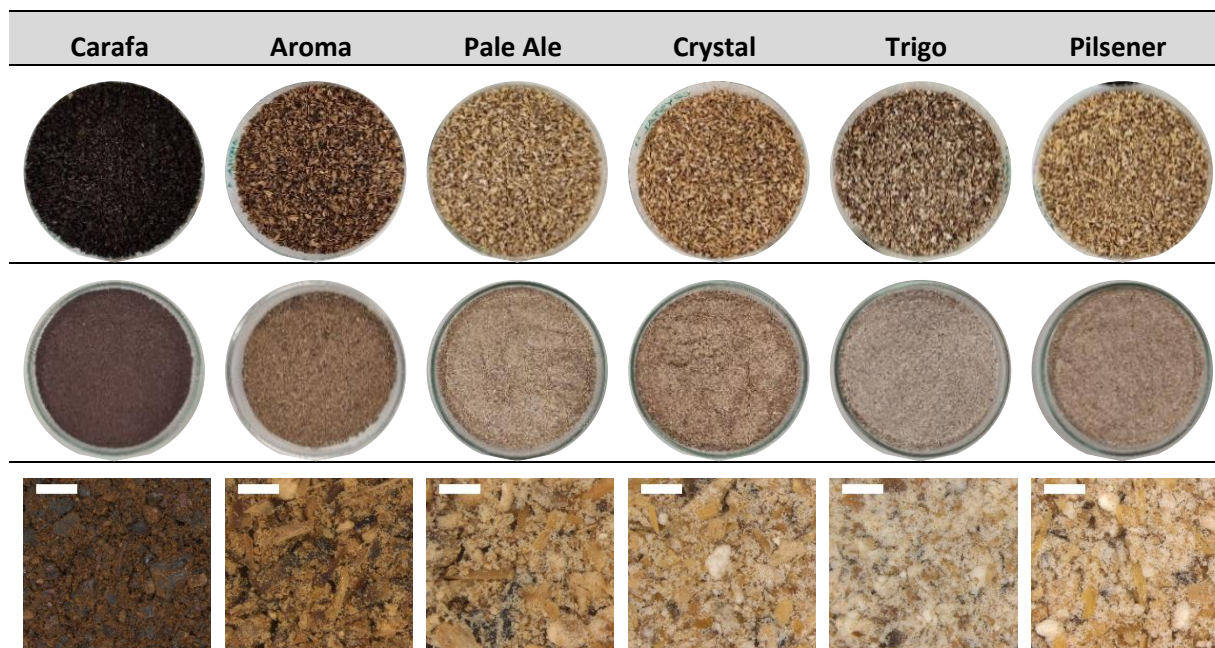


Table 3.3. Macroscopic appearance of the milled and grinded malts and microscopic images of the obtained powders. Scale bar represents 1 mm.



3.2. Proximate analysis

Ash yield (A), volatile matter (VM) and moisture (M) contents of the BSGs were measured according to the standardized procedures described in ISO 18122:2016 (Solid Biofuels – Determination of ash content) [32], ISO 18123:2016 (Solid biofuels – Determination of the content of volatile matter) [33], and ISO 18134-1:2016 (Solid biofuels – Determination of moisture content – Oven dry method – Part 1: Total moisture – Reference method) [34], respectively. The fixed carbon (FC) was determined by difference of these values:

$$FC(\%) = 100 - M(\%) - VM(\%) - Ash(\%) \quad (3.1)$$

The content of moisture (M) was gravimetrically determined by means of equation (3.2) using a vacuum oven Heraeus Vacutherm shown in **Figure 3.1.(a)**.

$$M(\%) = \frac{m_0 - m_d}{m_0} \cdot 100 \quad (3.2)$$

where m_0 is the initial mass of the original sample and m_d is the mass of the dry sample, after two hours in vacuum oven at 105 °C (the content were manually mixed after the first hour) .

Volatile matter (VM) and ash (A) were also gravimetrically determined using the muffle furnace Heraeus Thermo M-104, represented in **Figure 3.1. (b)**. In this case, equations (3.3) and (3.4) were used for the volatile matter (VM) and ash (A) calculations, respectively.

$$VM(\%) = \left(\frac{100 \cdot (m_0 - m_v)}{m_0} - H \right) \cdot \frac{100}{100 - H} \quad (3.3)$$

where m_0 is the initial mass of the original sample and m_v is the mass of the sample after volatilisation.

$$A(\%) = \left(\frac{m_a}{m_d} \cdot 100 \right) \cdot \frac{100}{100 - H} \quad (3.4)$$

where m_d is the mass of the dried sample and m_a is the mass of the remnant matter.

In **Figure 3.2.** are illustrated the residues after the experiments for the determination of ash and volatile matter.



Figure 3.1. Vacuum oven (left) and muffle furnace (right) used in proximate analysis.



Figure 3.2. Alumina pan (a), residues of volatile matter (b) and residues after the experiment for the determination of ash (c).

3.3. Ultimate analysis

The chemical composition of BSG in terms of carbon (C), hydrogen (H), nitrogen (N), sulphur (S) and oxygen (O) was determined using a CHNS-O Thermo Flash 2000 elemental analyser, operating at 900 °C in an atmosphere of pure oxygen. The oxygen content was calculated by difference in a dry and ash-free basis according to the equation (3.5).

$$O(\%) = 100 - C(\%) - H(\%) - N(\%) - S(\%) \quad (3.5)$$

3.4. Calorific value

The higher heating value (HHV) was calculated applying the relationship of Channiwala and Parikh [35], through which it is possible to calculate the HHV of the samples, considering the content (%w/w) in carbon (%C), hydrogen (%H), oxygen (%O), sulphur (%S), nitrogen (%N) and ash (%A).

$$HHV \left(\frac{MJ}{kg} \right) = 0.3491 \%C + 1.1783 \%H + 0.1005 \%S - 0.1034 \%O - 0.0151 \%N - 0.0211 \%A \quad (3.6)$$

3.5. Thermogravimetric analysis (TGA)

Thermogravimetric analysis is defined by the ICTAC as “a technique in which the mass of the sample is measured as a function of temperature, while the sample is subjected to a controlled temperature programme” [36]. This analysis can be carried out either in a dynamic mode, by means of a heating programme at constant rate, or under isothermal conditions, as a function of time. In both cases the mass loss or the mass loss rate, that are directly related to the removal of volatile compounds or to a chemical process, are determined at every temperature or time. The basic components of this technique are both the mass control, and the thorough temperature control and are schematised in **Figure 3.3**.

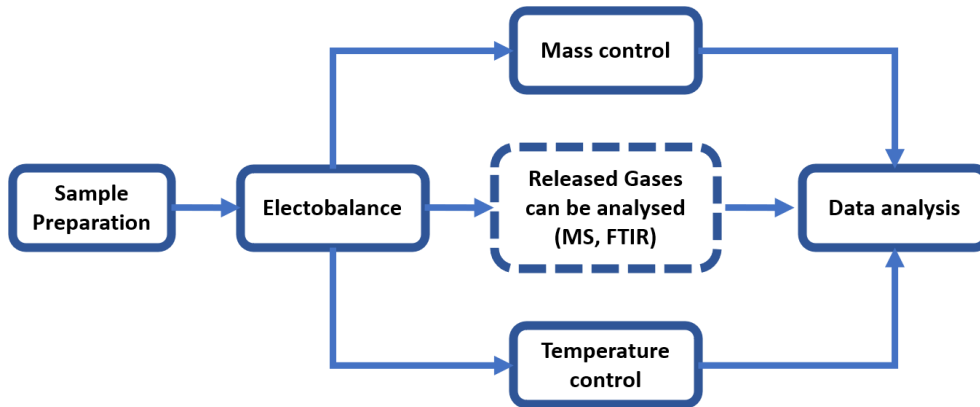


Figure 3.3. Basic components of the Thermogravimetric Analysis.

The results of thermogravimetric analysis are displayed in a thermogravimetric curve, also called thermogram. This consists of a sigmoidal curve with one or more stages, depending on the chemical nature of the components and the sample composition. A weight loss at low or moderate temperatures (up to 150 °C) corresponds to the loss of volatile components like water, organic solvents with low molecular weight, or absorbed gases. For temperatures in the range of 150-250 °C, the loss of low molecular weight components can be detected, such as additives, crystallisation water, plasticizers or even the first decomposition products at low temperatures. At temperatures higher than 225-250 °C, the thermal degradation is usually initiated. Its evolution is related to the atmosphere used during the measurement. At temperatures about 500 °C, hydrocarbonated compounds which thermal decomposition do not lead to the formation of volatile fragments, are charred. These remain as residues together with non-degradable fillers or inorganic additives.

If the measurement is performed under oxidant atmosphere, the char residue leads to the formation of gaseous carbon dioxide, and the inorganic residues remain as ashes of metallic oxides or of salts that cannot be oxidized. When the thermogravimetric analysis is carried out under oxygen or air atmospheres, it is called thermo-oxidative decomposition.

Thermogravimetric results can also be displayed as a differential curve or DTG curve that is obtained from the first derivative of the thermogravimetric curve. In the DTG curve, the drops with maximum slope of the thermogravimetric curve will correspond to the maxima of the differential curve. This technique allows the study of the thermal decomposition of polymers, the decomposition rate, the reaction order and the activation energy, but also allows the determination of additives and fillers present in complex formulations. Thermogravimetric analysis can be coupled to other complementary analytical techniques (Infrared Spectroscopy, Mass Spectrometry, etc.) to give information about the nature of the mass loss process. Such information will be useful for the elucidation of the mechanism of the degradation process, or for obtaining fundamental information about the material itself.

In this work, samples were analysed by a dynamic thermo-gravimetric procedure. Thermo-oxidative stability data were obtained by means of a Mettler-Toledo TGA 851 series represented in **Figure 3.4 (a)**. The samples, with a mass of about 3-6 mg were introduced in TGA Mettler-Toledo perforated alumina crucibles, with capacity of 70 μL (**Figure 3.4 (b)**) and the mentioned equipment was used for monitoring the mass loss (TG) and the differential weight loss (DTG) profiles. The thermogravimetric tests were performed from 25 to 800 $^{\circ}\text{C}$ at a heating rates of 2, 5, 10, 20, 30 $^{\circ}\text{C}/\text{min}$, under oxidative atmosphere of oxygen at a flow rate of 50 mL/min. Three specimens of each sample were analysed and the averages and deviations were considered as representative. The obtained results were evaluated by means of the STARe 9.10 software.



Figure 3.4. (a) Mettler-Toledo TGA 851 series and (b) 70 μL alumina capsules containing ash.

3.6. Kinetic analysis of the thermo-oxidative decomposition of biomass

As mentioned at the beginning of this work, through the application of thermogravimetric analysis (TGA) by means of non-isothermal multiple heating rates of a sample submitted to a controlled heating programme while temperature or time and mass loss are measured, it is possible to obtain important parameters for the design and optimisation of the energy valorisation process of a biomass.

The kinetic analysis is usually described by the kinetic triplet: activation energy (E_a), pre-exponential factor (A) and kinetic function ($f(\alpha)$).

In the following scheme in **Figure 3.5**, is illustrated the summary procedure for the calculation of the kinetic triplet.

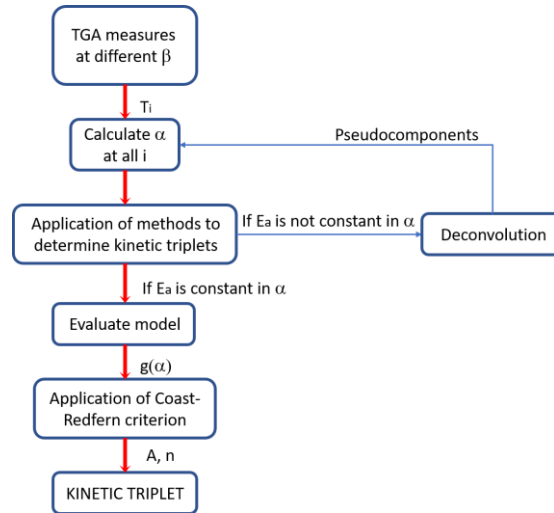


Figure 3.5. Procedure for the calculation of the kinetic triplet.

In order to describe the chemical changes occurring in the system, it is necessary to calculate the conversion rate at any time. With this aim, the thermal decomposition rate equation is used. The equation considers two different contributions: one that depends on the reactant concentration, and another one that depends on the absolute temperature, the reaction rate (k).

$$\text{Thermal decomposition rate} = f(\text{reactant concentration}) * k(\text{temperature})$$

Reaction rate is described by the Arrhenius equation:

$$k(T) = A * \exp\left(-\frac{Ea}{RT}\right) \quad (3.7)$$

Where R is the universal gas constant, T is the absolute temperature, Ea is the activation energy, A is the pre-exponential factor, that is assumed to be independent of temperature.

The reactant concentration present at every moment in the thermal decomposition process can be expressed, as suggested by Hirata [37], in terms of mass loss at every time (ω). In this case, the function that depends on the concentration will be ω , and the kinetic equation will be:

$$\frac{d\omega}{dt} = -\omega * A * \exp\left(-\frac{E}{RT}\right) \quad (3.8)$$

The kinetic equation can also be determined by defining the reactant concentration by means of the conversion. The degree of conversion, α (or decomposition degree) can be defined as the sample mass lost at a time t , divided by the sample mass that would be lost at infinite time or total mass loss:

$$\alpha = \frac{\omega_0 - \omega}{\omega_0 - \omega_\infty} \quad (3.9)$$

Where ω , ω_0 , ω_∞ are the actual (at time t), the initial and final mass of the sample, respectively.

Thus, the rate equation will be given by:

$$\frac{d\alpha}{dt} = f(\alpha) * k(T) = f(\alpha) * A * \exp\left(-\frac{E}{RT}\right) \quad (3.10)$$

where $f(\alpha)$ depends on the mechanism of the degradation reaction.

In **Table 3.4** are shown some of algebraic functions usually used to express the differential function $f(\alpha)$ and its integral function $g(\alpha)$. A complete explanation between theoretical decomposition mechanisms and their mathematical models can be found in literature [38].

These functions help to develop a model for thermal and thermo-oxidative decompositions in full-scale systems. It is known that each single reaction step is representative of a complex network of reactions, but the aim of these functions is to describe the behaviour of the reaction in terms of an intrinsic kinetics through a simplified reaction pathway, in which heat and mass transfer limitations are not considered.

Table 3.4. Algebraic expressions for the differential $f(\alpha)$ and integral $g(\alpha)$ functions for most frequently used mechanisms of solid-state processes

Symbol	$f(\alpha)$	$g(\alpha)$	Solid-state processes
Sigmoidal curves			
A_2	$2(1 - \alpha)[- \ln(1 - \alpha)]^{-1}$	$[- \ln(1 - \alpha)]^{1/2}$	Nucleation and growth (Avrami equation 1)
A_3	$3(1 - \alpha)[- \ln(1 - \alpha)]^{-1/2}$	$[- \ln(1 - \alpha)]^{1/3}$	Nucleation and growth (Avrami equation 2)
A_4	$4(1 - \alpha)[- \ln(1 - \alpha)]^{-1/3}$	$[- \ln(1 - \alpha)]^{1/4}$	Nucleation and growth (Avrami equation 3)
Deceleration curves			
R_1	1	α	Phase boundary controlled reaction (one-dimensional movement)
R_2	$2(1 - \alpha)^{1/2}$	$[1 - \ln(1 - \alpha)^{1/2}]$	Phase boundary controlled reaction (contracting area)
R_3	$3(1 - \alpha)^{2/3}$	$[1 - \ln(1 - \alpha)^{1/3}]$	Phase boundary controlled reaction (contracting volume)
D_1	$1/(2\alpha)$	α^2	One-dimensional diffusion
D_2	$-1/\ln(1 - \alpha)$	$(1 - \alpha)\ln(1 - \alpha) + \alpha$	Two-dimensional diffusion
D_3	$\frac{3(1 - \alpha)^{2/3}}{2 \left[1 - (1 - \alpha)^{1/3}\right]}$	$\left[1 - (1 - \alpha)^{1/3}\right]^2$	Three-dimensional diffusion
D_4	$\frac{3}{2} \left[(1 - \alpha)^{-1/3} - 1\right]$	$\left[1 - \left(\frac{2}{3}\right)\alpha\right] - (1 - \alpha)^{2/3}$	Three-dimensional diffusion
F_1	$1 - \alpha$	$-\ln(1 - \alpha)$	Random nucleation with one nucleus on the individual particle
F_2	$(1 - \alpha)^2$	$1/(1 - \alpha)$	Random nucleation with two nuclei on the individual particle
F_3	$\frac{1}{2}(1 - \alpha)^3$	$1/(1 - \alpha)^2$	Random nucleation with three nuclei on the individual particle

3.6.1. Calculation of the activation energy

There exist different methods to calculate the activation energy E_a , depending on the assumption of setting a particular kinetic function, the analysis at single or multiple heating rates, or the mathematical

treatment of the general kinetic law, in terms of differential or integral approach. A short revision of methods used in this work is given below:

Linear methods for the determination of the activation energy based on multiple thermogravimetric experiments at different heating rates and at a specific conversion degree

In this section it is proposed the single- α differential method (equation (3.11)), by H.E. Kissinger [39]. The method considers only one specific conversion degree, the maximum one. From the result of thermo-gravimetric analysis, if $\frac{d\alpha}{dt}$ against the temperature is plotted, it shows that, the decomposition rate raises until it gets a maximum value, and then it decreases to zero once the reactant is finished. At the maximum decomposition rate corresponds a temperature T_m that graphically corresponds to the inflection point in the thermogravimetric curve.

$$\ln\left(\frac{\beta}{T_m^2}\right) = -\frac{E}{RT_m} + \ln\left(-\frac{AR}{E} * f'(\alpha_m)\right) \quad (3.11)$$

where α_m is the maximum conversion.

According to the Kissinger's method, the activation energy can be calculated from the slope of the plots $\ln\left(\frac{\beta}{T_m^2}\right)$ versus $\left(\frac{1}{T_m}\right)$, for distinct experiments at constant heating rate β . Hence, the activation energy can be determined without knowing the reaction mechanism.

Linear methods for the determination of the activation energy based on multiple thermogravimetric experiments at different heating rates and at a several conversion degrees

However, it was demonstrated that the kinetic parameters may change during decomposition. In order to consider this variation isoconversional methods can be employed. They use data from different multi-linear non-isothermal experiments and do not take model assumptions for the analysis. Isoconversional methods can be integral or differential [40].

Integral methods are based on an estimated integration of the integral function of conversion $g(\alpha)$. According to the different assumptions, different methods were proposed.

J.H. Flynn, L.A. Wall [41] and Ozawa [42] (FWO) proposed the following multiple- α method for the determination of activation energy:

$$\log \beta = \log \frac{EA}{R * g(\alpha)} - 2.315 - \frac{0.457 E}{RT} \quad (3.12)$$

The activation energy for different conversions can be calculated from the slope of the plots of $\log \beta$ versus $\frac{1}{T}$ plotted at different α .

Using similar approaches Kissinger-Akahira-Sunose (KAS) proposed this equation:

$$\left[\ln\left(\frac{\beta}{T^2}\right)\right]_y = \ln\left(\frac{A_\alpha * R}{E\alpha_\alpha * g(\alpha)}\right) - \frac{E\alpha_\alpha}{R} * \left[\frac{1}{T}\right]_x \quad (3.13)$$

The activation energy at each conversion degree is calculated from the slope of the plots of $\ln\left(\frac{\beta}{T^2}\right)$ versus $\frac{1}{T_\alpha}$.

Friedman [43], using a differential approach, proposed the following equation:

$$\left[\ln\left(\frac{d\alpha}{dt}\right)_\alpha \right]_y = \ln(A_\alpha * f(\alpha)) - \frac{E_{a\alpha}}{R} * \left[\frac{1}{T_\alpha} \right]_x \quad (3.14)$$

The activation energy at each conversion degree can be calculated from the slope of the plots of $\ln\left(\frac{d\alpha}{dt}\right)_\alpha$ versus $\frac{1}{T_\alpha}$ at different α .

In all presented isoconversional methods, the determination of the activation energy is achieved without knowing the reaction mechanism.

3.6.2. Analysis of the kinetic function

There exist different methodologies to obtain the kinetic function, in this work Master-Plots (MP) were used. These are reference theoretical curves ($M-P_t$) that depend on the kinetic model, but that are generally independent of the kinetic parameters of the process. The experimental TGA data can be transformed into experimental curves ($M-P_e$), and a comparison between them and $M-P_t$ allows the selection of the appropriate kinetic model of the process under investigation or, at least, helps to reduce the span of suitable kinetic models.

There exist three main types of reference theoretical curves, those based on the differential form ($M-P_f$) of the generalized kinetic equation, those based on the integral form ($M-P_g$) and also combination of both differential and integral forms ($M-P_{fg}$). These curves are usually reduced at $\alpha = 0.5$ for better visualization and this procedure is also known as Criado method [44].

Once the activation energy is determined by one of described isoconversional methods, the Criado method allows the determination of the kinetic model.

The kinetic analysis of non-isothermal process is typically carried out employing a single step kinetic equation:

$$\frac{d\alpha}{dt} \equiv \beta * \frac{d\alpha}{dT} = A * f(\alpha) * k(T) = A * f(\alpha) * e^{-\frac{E_a}{RT}} \quad (3.15)$$

The integration of this last equation leads to the inverse integral kinetic function $g(\alpha)$:

$$g(\alpha) = \int_0^\alpha \frac{d\alpha}{f(\alpha)} = \frac{A * E_a}{\beta * R} * \int_0^\infty \frac{e^{-x}}{x^2} = \frac{A * E_a}{RT} * p(x) \quad (3.16)$$

Where $x = \frac{E}{RT}$ and $p(x) = \frac{e^{-x}}{x^2} * \sum_n \frac{n*(1-n)}{x+2*(n+1)}$ that is the result of Senum-Yang approximation.

In this work the Senum-Yang approximation was truncated at the fifth term since it permits to obtain a good approximation (deviation lower than $10^{-8}\%$) with respect to exact temperature integral for $x > 10$ [45], condition always respect in this work.

Once the kinetic function and its inverse integral function were calculated from the experimental TGA results and previously calculated activation energy, the curve obtained plotting experimental curves ($M-P_e$) at different α permits the graphic comparison of the those with the theoretical reduced master curves. This procedure provides an easy and accurate method for the determination of the reaction mechanism. In **Figure 3.6.** are shown the Master-Curves present in **Table 3.4,** both in differential and integral form.

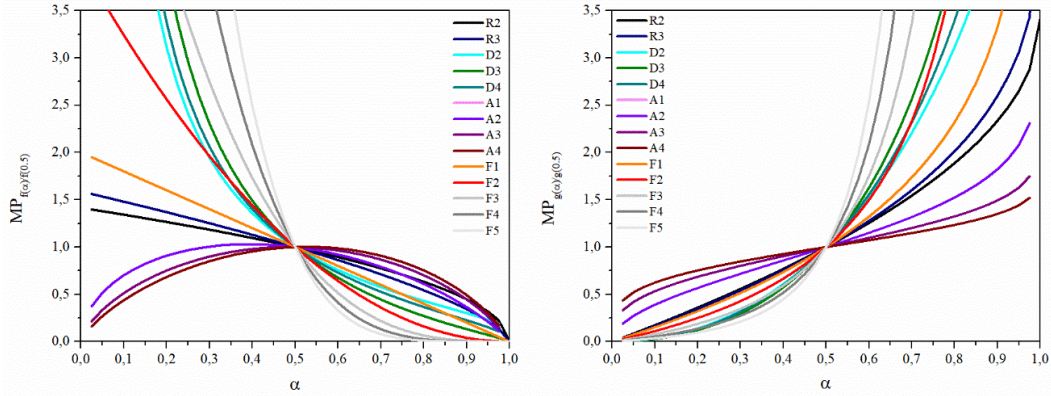


Figure 3.6. Criado master curves for some of the kinetic models shown in **Table 3.4.**

3.6.3. Analysis of the pre-exponential factor

In order to complete the kinetic triplet, the pre-exponential factor A has to be found. For that, the Perez-Maqueda *et al* criterion ($P-Mc$) [46] has to be accomplished; that is, the independence of the activation parameters E_a , A on the heating rate β . This criterion is usually employed with E_a and A invariable with the aid of Coats-Redfern's equation [47]:

$$\left[\ln \frac{\beta * g(\alpha)}{T^2} \right]_y = \ln \frac{AR}{E_a} + \frac{E_a}{R} * \left[\frac{1}{T} \right]_x \quad (3.17)$$

Knowing activation energy from previously isoconversional methods and once the most suitable mechanism was determined using master plots, Perez-Maqueda criterion was applied and the best n order of the kinetic model was determined by minimizing equation (3.18). The points $\{x, y\}$ calculated applying equation (3.17) should lie on the same straight line to all heating rates once the best n is calculated. The pre-exponential factor (A) is calculated by averaging the values A_β from the intercept at $y = 0$ of the Coats-Redfern equation.

$$\xi(n, \alpha) = \sum_i^h \left| (-R) * \frac{d}{dT} \left(\frac{\ln(\beta_i * T^{-2} * g(\alpha))}{T^{-1}} \right) - E_{a_{iso}} \right| \quad (3.18)$$

3.7. Combustion of BSGs in a pilot incineration plant

As a validation approach, the dry beer spent grains (BSGs) of the different malt varieties were pelletised together in a Smart Wood PLT-50 setup, with a production capacity of 20-30 kg/h. Pellets with a diameter of 6 mm and a length of 30 mm were obtained, which morphology is shown in **Figure 3.7**. Afterwards, they were subjected to combustion for 1 h at temperatures in the range from 400 to 700 °C in steps of 50 °C in a Thermo Heraeus M-104 muffle furnace, to validate the ash yields and appearance after combustion.

Finally, 1 kg of the pelletised BSGs was applied in an own-designed pilot incineration plant, such as that shown in **Figure 3.7**. The setup was equipped with a hopper with a base square 0.5 m length and inclined walls together with a cylindrical bar to promote vibrations to prevent blocks. The feeding flow was controlled by a rotary valve with a diameter of 4.86 cm, previously calibrated. Then, the conveyor belt with dimensions of 4.55 m length, 0.15 m wide, and spaced partitions every 0.175 m, allows the transport of the pellets to the feeding tube regulated by a rotary valve and subsequently to the incineration unit. The incineration unit consists of a combustion chamber with a moving grill in a circular motion to prevent potential slagging. Inside this chamber, two ignition glow plugs with lengths 140 mm and 250 W each are installed, and four temperature sensors monitor the temperature of the top, gas outlet, the heart of the combustion chamber, and ashes collector. Air is conveyed from the downstream of the combustion chamber to ensure combustion and extract fumes from the chamber. Ashes are recovered into a tray located at the bottom of the chamber, with dimensions of 19×30.4×9.4 cm³. The tightness of the chamber was ensured with an isolated door that included a viewing port. Overall, the operating conditions were feeding rate of about 1 kg/h and airflow of 50 L/min (21% O₂), to assure combustion temperatures above 500 °C during operation. Once the mentioned amount of pellet was consumed, the remnant ash was collected and the yield and apparent density were calculated.



Figure 3.7. Pellets of beer spent grains (BSG) and incineration pilot plant.

4. RESULTS AND DISCUSSION

In this section are presented the results obtained for the six different types of mashed malts (Carafa, Aroma, Pale Ale, Trigo, Pilsener and Crystal) and for the two different brewer's spent grains (ORISC and WHEAT). All analysed biomasses could be associated to real by-products of the brewery industry. Although beer plants usually use blended malts to obtain beer wort, in this work the mashed malts were considered as the starting point for the preliminary study and for the understanding the behaviour of ORISC and WHEAT brewer's spent grain (BSG), consisting in mixtures of some of the studied malts. This section is structured according to **Figure 4.1** and involves the biomass characterisation, the thermo-oxidative stability evaluation followed by the apparent energy calculation, kinetic function assessment and pre-exponential factor determination.

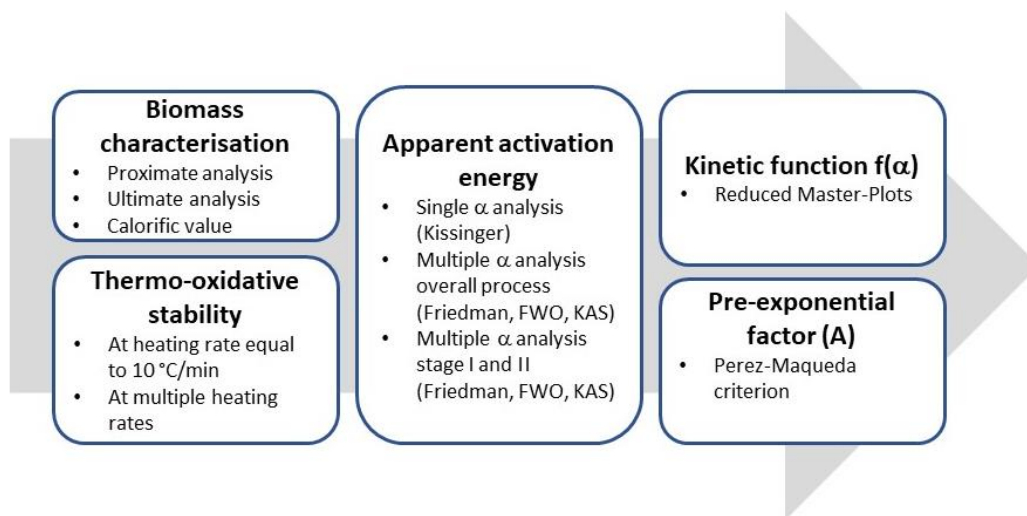


Figure 4.1. Scheme for the results evaluation in the current study.

4.1. Biomass sample analysis

The study of biomasses started with the characterization of malts and BSGs through proximate and ultimate analysis, then on the base of the results of these two, the calorific values were calculated.

4.1.1. Proximate analysis

The evaluation of the moisture, volatiles, fixed carbon and ash yield by means of the proximate analysis brings valuable information for the initial characterisation of the raw malts of this study. According to the obtained results, the behaviour of these biomass sources can be validated as solid biofuels. **Table 4.1** summarizes the results of proximate analysis of the different malt varieties and BSGs. All tests were repeated twice and the values on the table are the result of the average.

Table 4.1. Proximate analysis results of biomass samples.

<i>Proximate Analysis (wt. %)</i>								
	<i>Aroma</i>	<i>Carafa</i>	<i>Pale Ale</i>	<i>Pilsener</i>	<i>Crystal</i>	<i>Trigo</i>	<i>ORISC</i>	<i>WHEAT</i>
Moisture %	0.6	0.7	0.4	1.1	1.2	0.8	1.3	0.8
Volatiles %	91.8	88.3	95.3	92.2	86.6	95.6	82.7	83.3
Ash yield %	1.7	5.4	2.3	2.1	1.7	2.5	4.3	2.5
Fixed Carbon %	5.9	5.5	2.0	4.6	10.4	1.2	11.7	13.4

Overall, the proximate analysis shows similar percentages of moisture, volatiles, ash yield and fixed carbon for all samples. More in details, the applied drying procedure permitted to obtain very low water content both for malts and BSGs. Volatile content was similar among the malts and slightly lower for the ORISC and WHEAT BSGs. Moreover, the small difference in the volatiles between the ORISC and WHEAT may be mainly due to the different content of remnant humidity, which will determine this calculation. Ash yield is around 2% in all the malts except in Carafa, in which it was significantly higher. This result probably causes the difference in ash yield between BSGs, since ORISC type contains a certain percentage of Carafa malt. Indeed, the ORISC showed almost double ash yield than the WHEAT mixture.

4.1.2. Ultimate analysis

Ultimate analysis permits to obtain the content of carbon, hydrogen, nitrogen and sulphur. **Table 4.2** shows the results obtained for malts and BSGs.

Table 4.2. Ultimate analysis results of biomass samples.

<i>Ultimate Analysis (wt. %)</i>								
	<i>Aroma</i>	<i>Carafa</i>	<i>Pale Ale</i>	<i>Pilsener</i>	<i>Crystal</i>	<i>Trigo</i>	<i>ORISC</i>	<i>WHEAT</i>
Carbon %	44.7	46.7	44.6	44.0	44.4	44.4	45.3	46.0
Hydrogen %	6.4	6.4	6.6	6.4	6.4	6.6	6.8	6.8
Nitrogen %	1.6	2.6	1.9	1.4	1.4	2.1	4.0	3.3
Sulphur %	0	0	0	0	0	0	0	0
Oxygen %	47.3	44.3	46.9	48.2	47.8	46.9	44.0	43.8

*Oxygen percentage calculated by difference.

Overall, BSGs show higher content of Carbon and Nitrogen, while hydrogen content resulted almost equal. Looking at the values reported in table, it should be noticed the high value of carbon content for both BSGs and malts. This high percentage of C implies high values of calorific value and, from the point of view of energy production, it implies their suitability for being used in thermo-chemical conversion processes. Moreover, a null content of sulphur was found for all analysed biomasses.

Even looking at the nitrogen content, it should be appreciated its low content for all biomasses. This result would suggest the improbable production of unwanted NO_x compounds during combustion. This

observation together with the null Sulphur content and the low percentages of ash yield found in previous section, promote the use of these materials in the production of bioenergy.

4.1.2. Calorific value

Exploiting the values obtained by ultimate and proximate analysis, the high heating values (HHV) of biomasses were calculated applying Channiwala and Parikh equation. The results obtained are gathered in **Table 4.3**.

Table 4.3. Higher heating value of biomasses calculated with the relationship of Channiwala and Parikh.

<i>Calorific value (MJ/kg)</i>	
	<i>HHV</i>
<i>Aroma</i>	18.2
<i>Carafa</i>	19.1
<i>Pale Ale</i>	18.4
<i>Pilsener</i>	17.8
<i>Crystal</i>	18.1
<i>Trigo</i>	18.3
<i>ORISC</i>	19.1
<i>WHEAT</i>	19.5

Comparing BSGs and mashed malts, it was found that malts revealed slightly lower HHV. This difference can be mostly due to the different content in Carbon. As expected, the HHV of both ORISC and WHEAT are almost equal and, in general, their value is higher than agri-food and agricultural residues, which value is around 15 MJ/kg [1], [48], [49].

4.2. Thermo-oxidative stability

In this section thermo-gravimetric analysis at a single heating rate (10 °C/min) and at different heating rates were performed in order to study the behaviour of mashed malts and BSGs during thermo-oxidative conditions. The temperature of peaks, the mass loss in the different regions and the onset/endset temperatures were assessed along with the zero-decomposition temperatures, by which it is possible to approximate the behavior of sample when heating rate tends to zero, avoiding the influence of the dynamic heating program.

4.2.1. Thermo-oxidative stability at a single heating rate

The thermo-oxidative stability was firstly assessed for all the samples by means of thermogravimetric analyses at heating rate of 10 °C/min in oxidative atmosphere. The obtained thermogravimetry (TG) and its first derivative (DTG) curves are shown in **Figure 4.2** The TG and DTG curves obtained were furtherly analyzed, and the onset and endset degradation temperatures (T_o , T_e), the peak temperature (T_p) and the mass loss percentages for the different stages (Δm) were obtained, which values are gathered in **Table 4.4**.

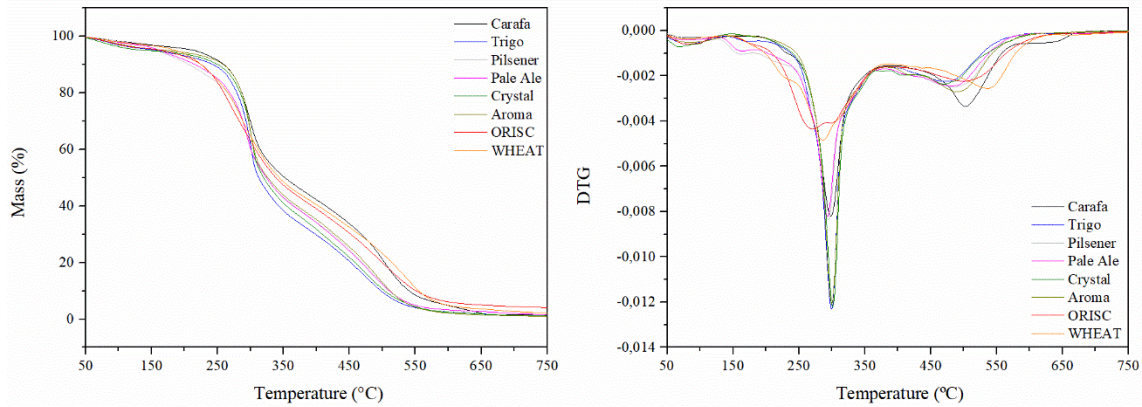


Figure 4.2. Thermogravimetry (TG) and its derivative (DTG) curves of malt and ORISC samples under oxidative conditions at heating rates of 10 °C/min.

The decreasing trend in the TGA curve shows the mass loss occurred during heating. Indeed, the resulting thermograms showed different mass-loss regions. The initial mass reduction, with a contribution of 2.8-5.1% from 25 °C to almost 170-180 °C, is due to remnant moisture vaporization. This step is followed by a second stage of decomposition, with a mass loss in the range from 52.8 to 61.9% that goes from almost 170-180 °C to 350-415 °C, due to devolatilization of volatile hydrocarbons from decomposition of hemicellulose, cellulose and lignin. The last decomposition, above 400 °C may be due to decomposition of lignin and char. In this last stage, the degradation continues quite fast until temperatures of 500-600 °C are reached. After that, degradation continues very slow until the end of the assay. Finally, the obtained residues were in the range from 0.1 to 4.6%. This low residue percentage is connected to the low ash yield found in previous sections. Overall, this behaviour has been previously reported for this kind of biomasses [51].

Table 4.4. Onset and endset degradation temperatures (T_o , T_e), peak temperature (T_p) and mass loss percentages for the different decomposition stages (Δm) obtained at $\beta=10$ °C/min.

	T_o (°C)	T_{p0} (°C)	Δm_0 (%)	T_{p1} (°C)	Δm_1 (%)	T_{p2} (°C)	Δm_2 (%)	T_e (°C)
Carafa	265 ± 1	91 ± 1	3.2 ± 1	299 ± 1	52.8 ± 1	506 ± 3	42.5 ± 1	547 ± 5
Aroma	275 ± 1	86 ± 1	4.3 ± 1	300 ± 1	56.3 ± 1	492 ± 3	38.5 ± 1	534 ± 3
Crystal	275 ± 1	77 ± 8	5.1 ± 1	300 ± 1	56.7 ± 1	477 ± 6	37.0 ± 1	530 ± 3
Pale Ale	265 ± 1	91 ± 7	3.6 ± 1	294 ± 1	58.6 ± 1	481 ± 1	37.7 ± 1	528 ± 3
Trigo	273 ± 1	82 ± 1	4.5 ± 1	299 ± 1	61.9 ± 1	473 ± 1	32.5 ± 1	523 ± 3
Pilsener	259 ± 4	96 ± 5	2.8 ± 1	294 ± 1	58.4 ± 1	484 ± 1	37.5 ± 1	537 ± 3
ORISC	220 ± 3	82 ± 1	3.9 ± 1	273 ± 3	54.2 ± 1	499 ± 1	37.3 ± 1	566 ± 5
WHEAT	235 ± 1	79 ± 2	3.0 ± 1	286 ± 1	54.4 ± 1	537 ± 1	40.3 ± 1	585 ± 1

Non-significant differences were found in the onset temperature (T_o) for the different analysed varieties of malts. However, it must be highlighted the lowest onset decomposition temperature of the Pilsener malt, starting substantial mass-loss from 258 °C onwards. Both ORISC and WHEAT showed similar onset values at around 225 °C, quite lower than those of all analysed malts.

For the first mass loss region, assigned to remnant humidity, it must be emphasised the lower peak temperature (T_{p0}) and higher mass loss percentage (Δm_0) for the Crystal malt. Given that during this

stage free water is released, this observation could be correlated with a weaker water-biomass interaction and higher remnant humidity percentage.

The peak temperatures of the main decomposition stage (T_{p1}) remained unaltered and mass loss contributions were quite similar for all the samples. The only difference to be noted is in the Carafa malt, in which the mass loss in this main stage is a little lower than the average of malts and the temperature of the peak is higher than all other malts. Given that hemicellulose and cellulose are decomposed in this stage, it may be supposed a lower percentage of these components in this malt variety. The BSGs also behave similarly, mostly for mass loss results.

In the secondary decomposition stage, there are no significant changes among the samples, again except for the Carafa malt. The peak temperature was relatively higher than the other malts and the mass loss in this stage was also higher, suggesting a greater char production during combustion. This is also confirmed by the highest ash yield and lower volatiles content obtained in the proximate analysis. The shift to higher temperature of Carafa malt continues also in the endset temperature. Regarding the BSGs, the endset temperature of ORISC and WHEAT was slightly higher than malts, probably due to interactions between the different malt components that lengthened the decomposition process. In this last region, the WHEAT brewer's spent grains showed a slightly higher mass loss and peak temperatures were significantly displaced towards higher values.

4.2.2. Thermo-oxidative stability as a function of the heating rate

The thermo-oxidative stability was also analysed at different heating rates (β). In this section, thermogravimetric analyses were performed at β of 2, 5, 10, 20 and 30 °C/min. The resulting thermograms for malts and brewer's spent grain samples are shown in **Figure 4.3** and in **Figure 4.4**, respectively.

TGA and DTG curves clearly show the previously cited three main regions along the range of temperature. The remnant water release was followed by the decomposition of hemicellulose, cellulose, lignin and char.

As expected, increasing the heating rate, the curves were displaced to higher temperatures, both in TGA and DTG. The heating rate is known to affect both the shape of the TGA curve and the location of the maximum DTG peaks. This is because the temperature gradient between inside and outside is greater, which does not favour the decomposition of biomass. Moreover, there is less burning time so it is disadvantageous to burn out [48], [52].

The presence of shoulder/double peaks visible in all DTG curves means that multiple reactions are taking place at the same time. This behaviour is mostly noticeable when biomass is heated with a low heating rate programme while, the increase of the heating rate causes some peaks to merge and they are no longer distinguishable from each other. Indeed, some peaks are no longer present at high heating rates.

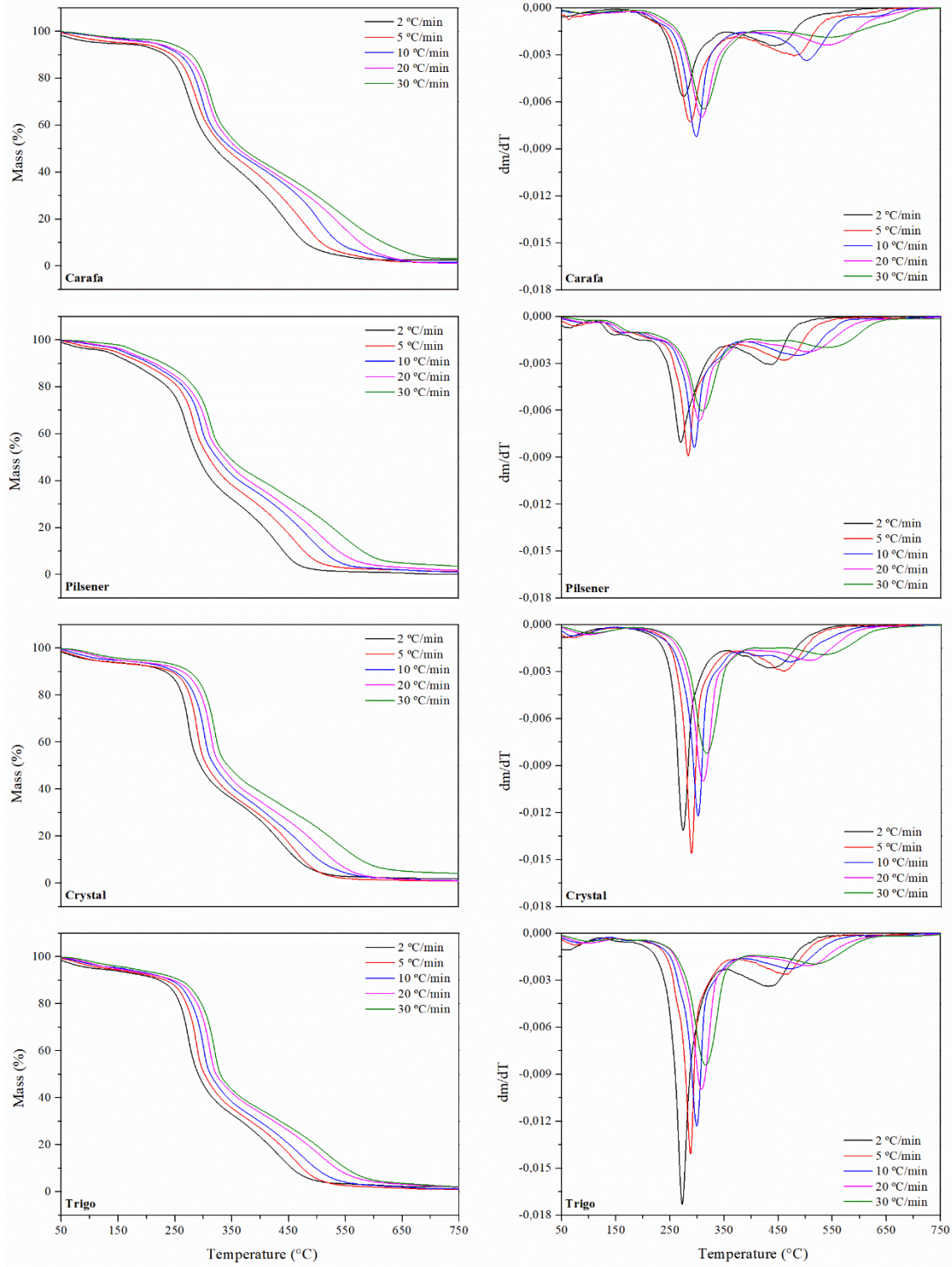


Figure 4.3. Thermograms of malt samples at different heating rates; 2, 5, 10, 20, 30 °C/min.

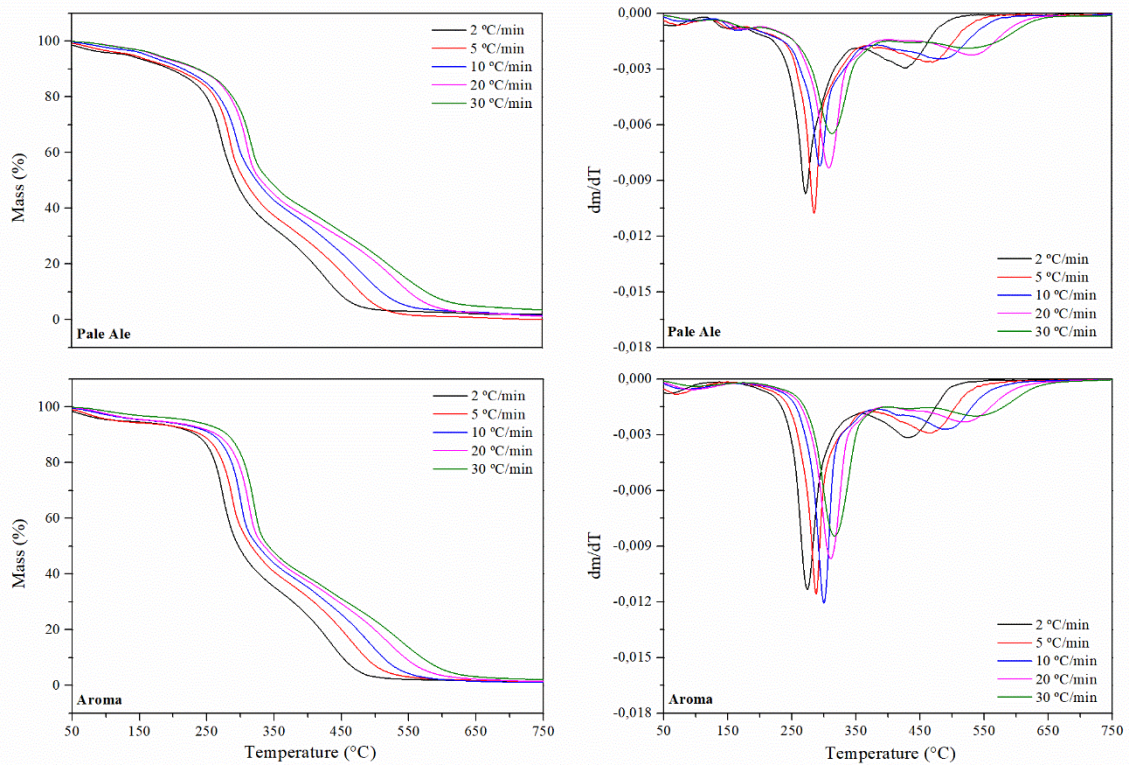


Figure 4.3. (continue) Thermograms of malt samples at different heating rates; 2, 5, 10, 20, 30 °C/min.

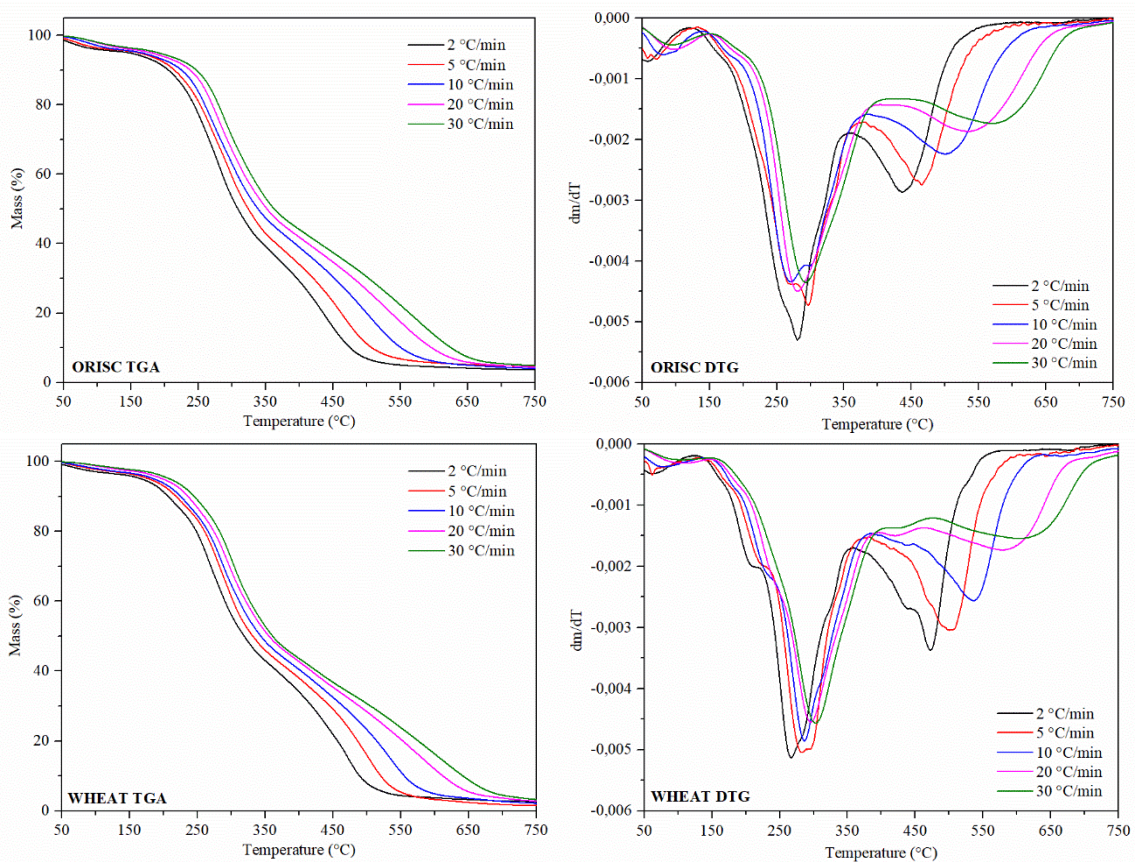


Figure 4.4. TGA (left) and DTG (right) of BSGs samples at heating rate equal to 2, 5, 10, 20, 30 °C/min.

The evolution of the characteristic decomposition temperatures for the two main stages (T_{p1} and T_{p2}) at all heating rates were assessed and results are plotted in **Figure 4.5** and **Figure 4.6**, for malts and BSGs, respectively. According to expectations, higher heating rates displaced the decomposition towards higher temperatures. Heat transfer during faster heating may be limited, and therefore, higher peak temperatures were found [48]. The evaluation of the zero-decomposition temperature (TDB) obtained when the heating rate tends to zero allows to avoid the influence of the dynamic heating program. The TDB can be therefore calculated adjusting the results to the exponential relationship shown in **Equation (4.1)**, where a , b and k are the parameters of the fitting. **Table 4.5** gathers the TDB values, the fitting parameters and the regression coefficients for both stages.

$$TDB(\beta) = \frac{a}{1 + b \cdot e^{-k \cdot \beta}} \quad (4.1)$$

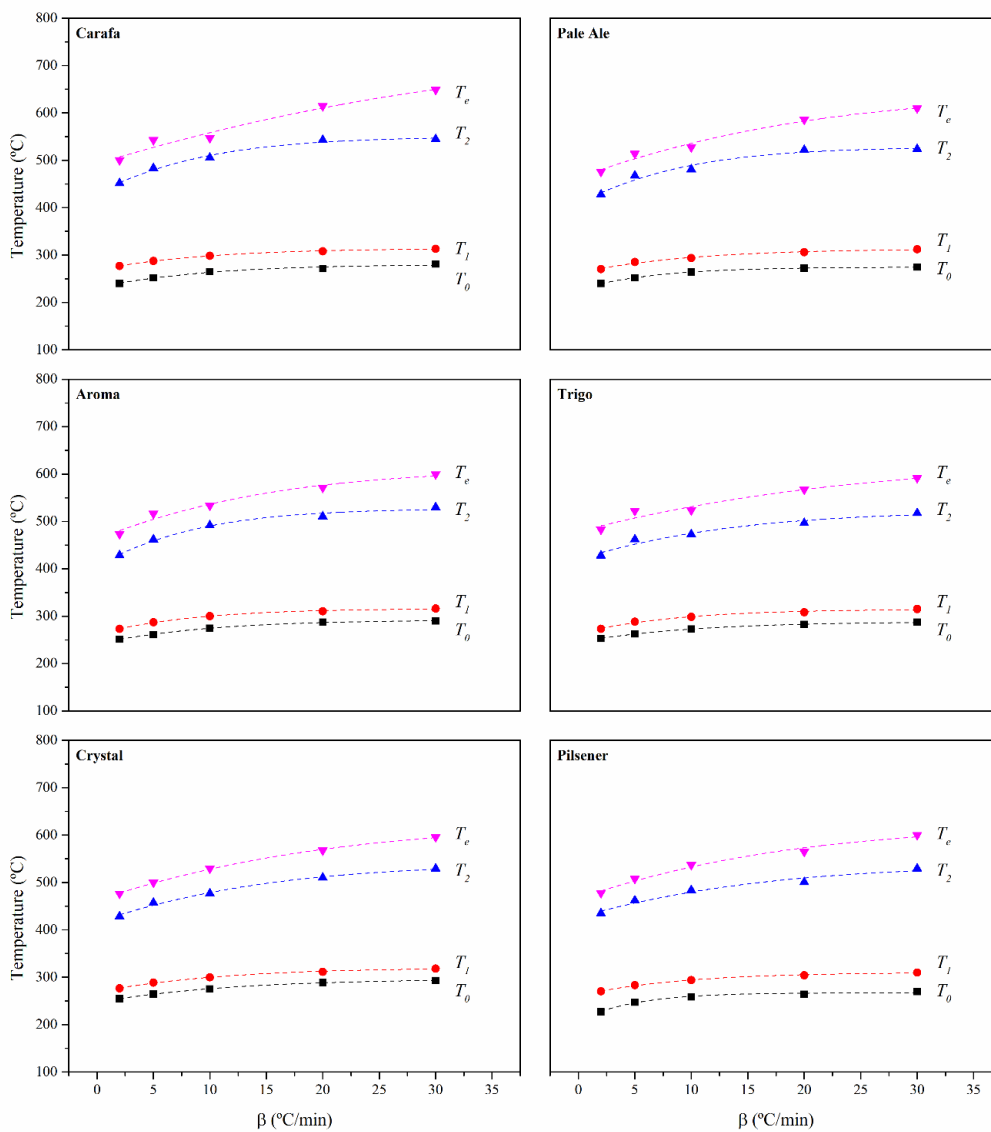


Figure 4.5. Evolution of the characteristic decomposition temperatures for the main stages (T_{p1} and T_{p2}) at all heating rates for malts.

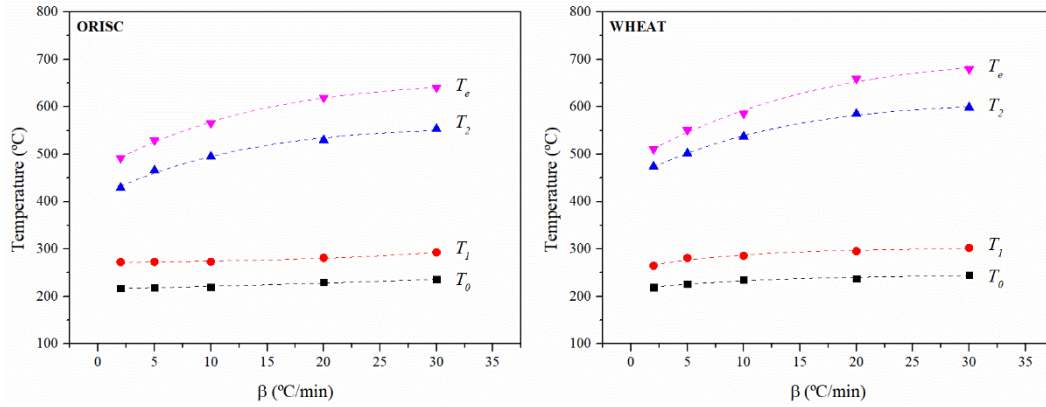


Figure 4.6. Evolution of the characteristic decomposition temperatures for the main stages (T_{p1} and T_{p2}) at all heating rates for both ORISC and WHEAT samples.

Table 4.5. TDB ($\beta \rightarrow 0$) values along with the fitting parameters and regression coefficient for both Stages I and II.

		TDB($\beta \rightarrow 0$) (°C)	<i>a</i>	<i>b</i>	<i>k</i>	<i>R</i> ²
Carafa	T_0	232	280 ± 4	0.21 ± 0.02	0.12 ± 0.03	0.962
	T_1	271	314 ± 1	0.16 ± 0.01	0.11 ± 0.01	0.996
	T_2	433	550 ± 7	0.27 ± 0.02	0.12 ± 0.03	0.978
	T_e	495	700 ± 63	0.49 ± 0.26	0.04 ± 0.03	0.940
Aroma	T_0	243	292 ± 1	0.20 ± 0.01	0.12 ± 0.01	0.997
	T_1	264	316 ± 2	0.20 ± 0.01	0.13 ± 0.01	0.993
	T_2	409	528 ± 8	0.29 ± 0.03	0.14 ± 0.03	0.972
Crystal	T_0	247	297 ± 1	0.20 ± 0.00	0.10 ± 0.00	0.998
	T_1	269	320 ± 2	0.19 ± 0.01	0.10 ± 0.01	0.992
	T_2	419	541 ± 12	0.29 ± 0.02	0.08 ± 0.02	0.984
	T_e	462	624 ± 10	0.35 ± 0.02	0.06 ± 0.01	0.997
Pale Ale	T_0	229	274 ± 1	0.20 ± 0.00	0.16 ± 0.01	0.999
	T_1	263	313 ± 4	0.19 ± 0.02	0.11 ± 0.03	0.976
	T_2	410	529 ± 12	0.29 ± 0.04	0.13 ± 0.05	0.939
Trigo	T_0	247	289 ± 1	0.17 ± 0.01	0.11 ± 0.01	0.993
	T_1	265	315 ± 3	0.19 ± 0.02	0.13 ± 0.03	0.976
	T_2	422	523 ± 20	0.24 ± 0.04	0.09 ± 0.05	0.920
	T_e	479	628 ± 75	0.31 ± 0.13	0.05 ± 0.04	0.901
Pilsener	T_0	212	267 ± 2	0.26 ± 0.04	0.22 ± 0.05	0.968
	T_1	263	310 ± 2	0.18 ± 0.01	0.12 ± 0.02	0.989
	T_2	428	539 ± 26	0.26 ± 0.05	0.07 ± 0.04	0.935
ORISC	T_0	215	254 ± 5	0.19 ± 0.50	0.01 ± 0.03	0.956
	T_1	266	269 ± 3	0.01 ± 0.01	0.06 ± 0.02	0.981
	T_2	412	560 ± 10	0.36 ± 0.03	0.1 ± 0.02	0.985
	T_e	472	656 ± 6	0.40 ± 0.01	0.09 ± 0.01	0.997
WHEAT	T_0	215	246 ± 5	0.14 ± 0.02	0.1 ± 0.05	0.919
	T_1	263	302 ± 5	0.17 ± 0.03	0.12 ± 0.05	0.919
	T_2	450	612 ± 6	0.36 ± 0.01	0.1 ± 0.01	0.996
	T_e	487	706 ± 19	0.45 ± 0.03	0.09 ± 0.02	0.987

4.3. Model-free kinetic analysis

In this section the use of model-free kinetic analyses was performed to assess the kinetic triplet: activation energies, reaction mechanism, pre-exponential factor. For this purpose, the results obtained by means of a set of experimental tests at different heating rates (2, 5, 10, 20 and 30 °C/min) were considered.

The activation energy was calculated by means of model-free methods considering single- α processes, as proposed by Kissinger, integral multiple- α methods, as described by Kissinger-Akahira-Sunose (KAS) and Flynn-Wall-Ozawa (FWO), and differential multiple- α models as the one proposed by Friedman.

The kinetic function $f(\alpha)$ for each biomass was determined by the use of reduced Master-Plots in which theoretical and experimental reduced curves were plotted to select the suitable approximation of reaction mechanisms. Once the mechanism of each sample was known, the pre-exponential factor was calculated using the Coast-Redfern equation by the application of Perez-Maqueda criterion.

4.3.1. Calculation of apparent activation energy

4.3.1.1. Single- α analysis

Kissinger method is a linear method for the determination of the activation energy based on multiple thermogravimetric experiments at different heating rates and at a specific conversion degree. It is based on the temperature at maximum decomposition rate (T_m) of the main stage of a given decomposition process. For this method, the $\ln(\beta/T_m^2)$ versus $1000/T_m$ (K^{-1}) were plotted in **Figure 4.7** for the malts and beer spent grains (BSGs) separately. The results were fitted to a linear behaviour and, using the slope of this line, it was possible to calculate the activation energy for each biomass. In **Table 4.6** are reported the activation energy calculated for the malts and BSGs.

The calculated activation energies were similar for all malts. Only the Carafa malt exhibited a higher activation energy with respect to the others. However, for the two BSG a huge difference was observed. Although reasonable values were obtained for the WHEAT sample, the ORISC revealed some inconsistencies. This dissimilar pattern was due to the limitation of Kissinger's method that only considers the temperature at the maximum decomposition point that, generally moves towards higher temperatures when the heating rate increases. A close look at the DTG curves of ORISC sample plotted in **Figure 4.4**, it showed that at the lower heating rates (2, 5, 10 °C/min), the main peak was composed by two different peaks near the maximum. It must be remarked that the T_m corresponds to the most intense point and, considering this double peak pattern, in some rates the most intense was the first, while in others the secondary was stronger. Therefore, the arbitrary variation of the maximum as a function of the heating rate, resulted in an incongruent approach. The failure of the method for this biomass can also be seen looking at the fitting lines; while for most of analysed samples the fitting lines have R^2 close to one, in the case of ORISC sample the fitting is very low. This behaviour demonstrates the limitations of the calculation of the activation energy from a single point at the temperature at the maximum decomposition rate.

In order to overcome this obstacle, the methods proposed by Friedman, FWO and KAS were applied, which consider the entire range of decomposition, not only T_m , and therefore, more accurate results may be obtained.

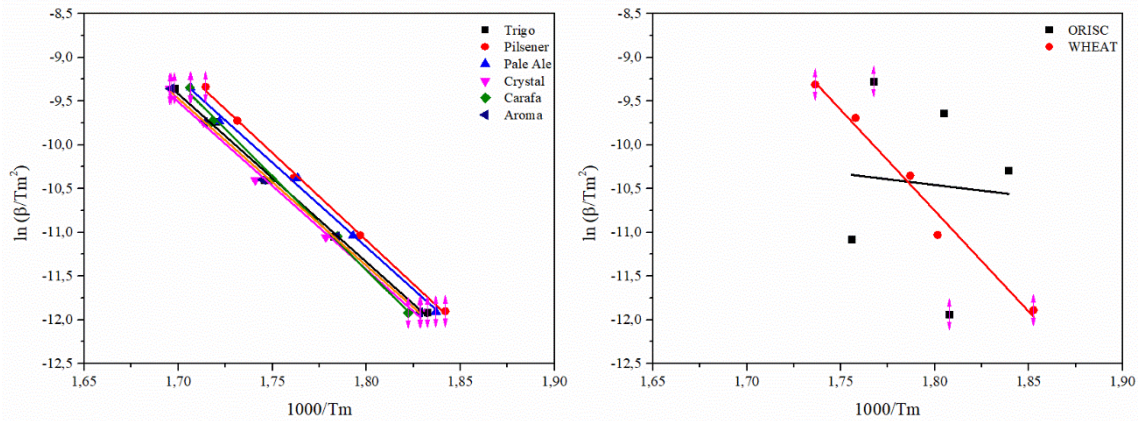


Figure 4.7. Kissinger plot for malts (left) and BSGs (right).

Table 4.6. Activation energy (E_a) calculated using Kissinger method based on maximum decomposition temperature T_m .

	$E_{aKissinger}$ (kJ/mol)
Carafa	179
Aroma	159
Crystal	159
Pale Ale	161
Trigo	160
Pilsener	166
ORISC	22
WHEAT	192

4.3.1.2. Multiple- α analysis for the global process

The iso-conversional methods proposed by Friedman, FWO and KAS are based on multiple thermogravimetric experiments at different heating rates and at a several conversion degrees. In this work the conversion degree (α) in the range 0.2-0.8 was considered representative for the kinetic analysis, since it is where the main process takes place and, therefore, considerations of heterogeneous and complex initiation and end-stage reactions are avoided.

The procedure to calculate the activation energy is similar to the one applied for Kissinger but in this case the slopes of the tendency lines drawn for each set of points were used to calculate the activation energy at each conversion degree ($E_{a\alpha}$). Moreover, these methods can be applied to the overall process or to a defined region of temperatures in which a specific peak or aggregation of peaks are studied. In the **Figure 4.8** and **Figure 4.9** are illustrated the linearized plots for these three iso-conversional methods for the malts and BSGs, respectively, considering the overall process. From the slopes of the fitting lines, the apparent activation energy was calculated as a function of α by means of the different methods and plotted in **Figure 4.10** and **Figure 4.11**.

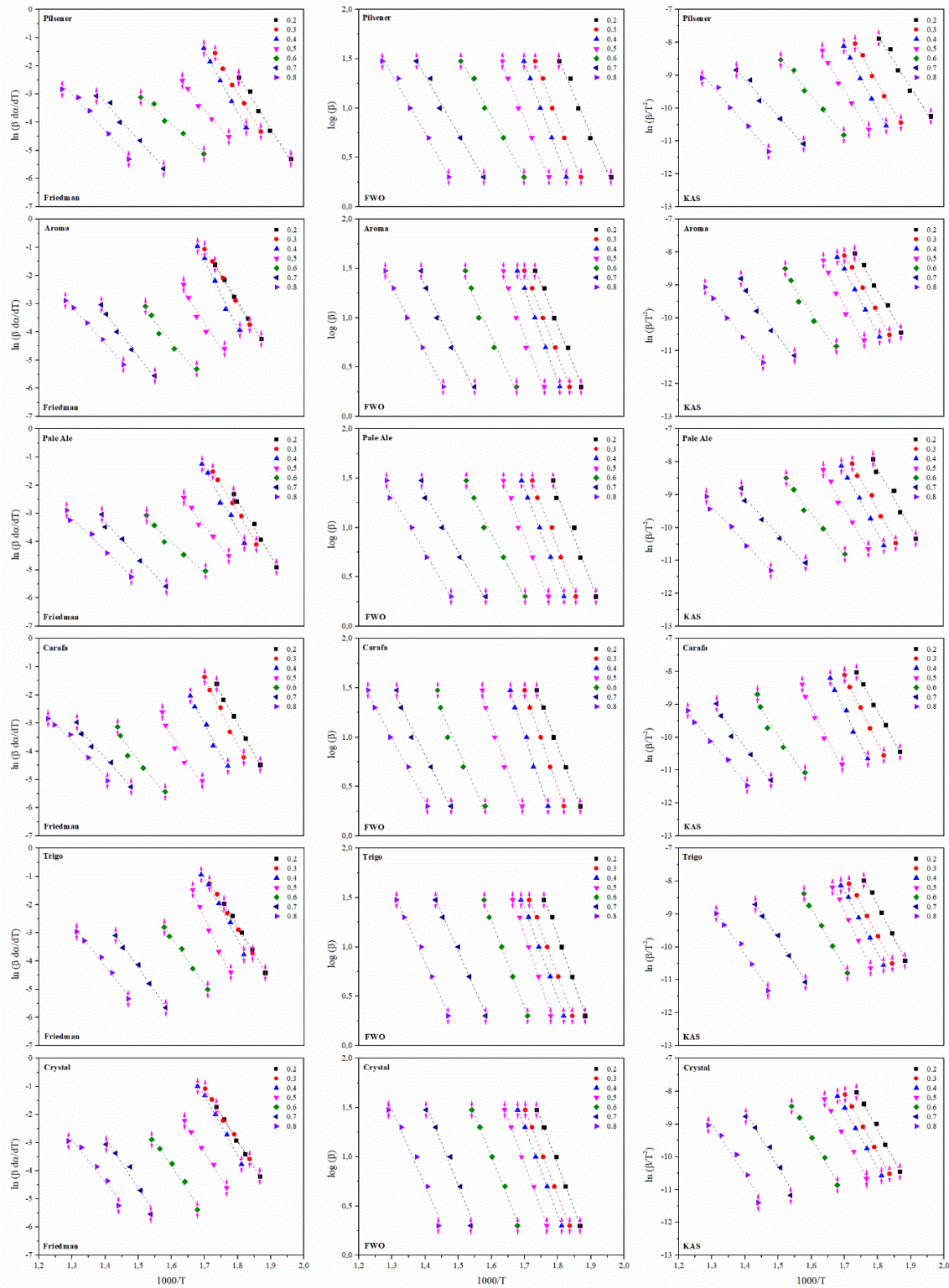


Figure 4.8. Friedman, FWO and FAS fitting plots of malts for different α considering the overall process.

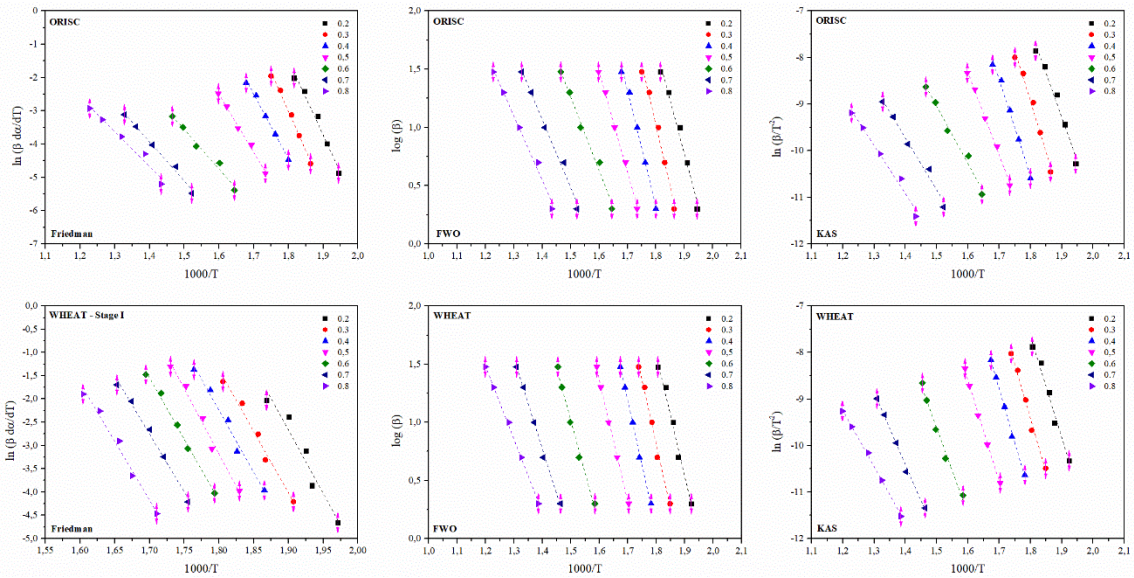


Figure 4.9. Friedman, FWO and FAS fitting plots of ORISC and WHEAT for different α considering the overall process.

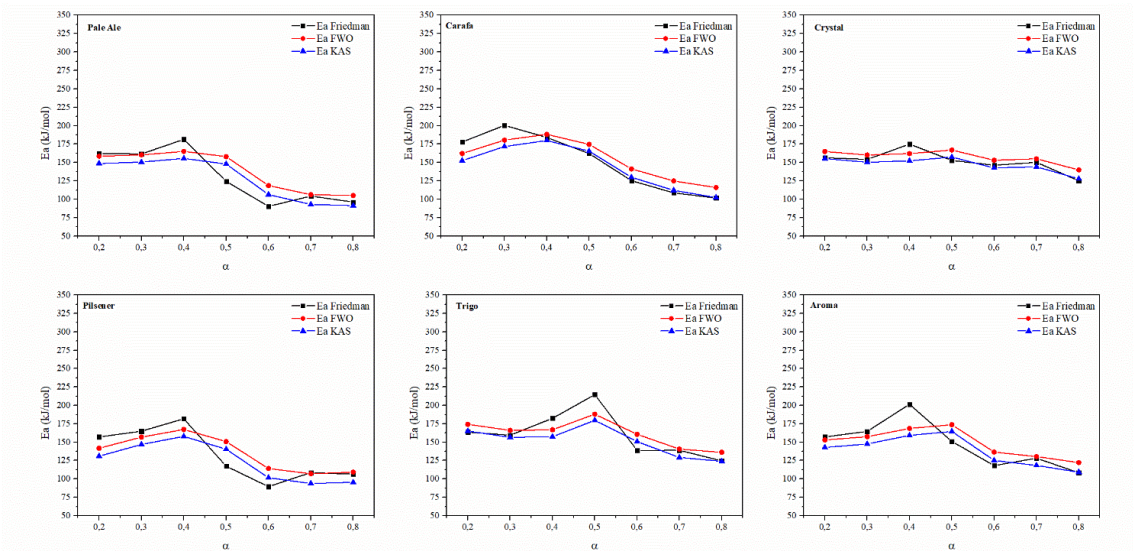


Figure 4.10. Evolution of apparent activation energy in the range of α 0.2-0.8 calculated with the different iso-conversional methods for malts.

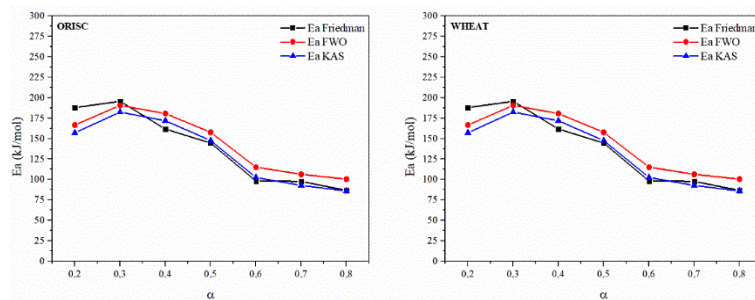


Figure 4.11. Evolution of apparent activation energy in the range of α 0.2-0.8 calculated with the different iso-conversional methods for ORISC and WHEAT samples.

The calculated apparent activation energy as a function of conversion revealed a non-constant behaviour. It was higher in for early-stage decomposition processes and decreased for higher conversion. Indeed, looking at DTG curves it is evident a net separation in stages and, it is manifested in almost all, a difference in the activation energy values at low and high α . This behaviour is more appreciable in BSGs samples (**Figure 4.11**), in which, at α in the range from 0.2 to 0.5, the value of activation energy was almost stable at values around 175 kJ/mol. Nevertheless, at α equal to 0.5-0.6 the activation energy started to decrease due to the “passage” from first to second main peak in DTG curves. After that, with α in the range from 0.6 to 0.8, the activation energy re-assumes a nearly constant value around 100 kJ/mol. From an overall perspective, the averaged values of E_a in the range of α from 0.2 to 0.8 are shown in **Table 4.7**.

Table 4.7. Apparent activation energy values obtained with the different iso-conversional methods considering the overall process.

Overall Process			
	$E_{a_{FWO}}$ (kJ·mol ⁻¹)	$E_{a_{KAS}}$ (kJ·mol ⁻¹)	$E_{a_{Friedman}}$ (kJ·mol ⁻¹)
Carafa	155 ± 24	145 ± 26	151 ± 34
Aroma	149 ± 16	138 ± 18	147 ± 25
Crystal	157 ± 7	147 ± 8	151 ± 9
Pale Ale	139 ± 25	128 ± 26	132 ± 32
Trigo	162 ± 14	152 ± 15	160 ± 23
Pilsener	135 ± 22	124 ± 23	132 ± 31
ORISC	145 ± 33	134 ± 35	139 ± 38
WHEAT	171 ± 27	162 ± 29	165 ± 37

Activation energy of malts was similar to average values, around 150 kJ/mol. Pale Ale and Pilsener malts have similar activation energy that is actually lower than the average, while Trigo variety has the activation energy higher than all the other malts.

For the BSGs, the mean activation energy of ORISC resulted always in the range of those of malts by which it is composed (Carafa, Aroma, Crystal and Pale Ale). On the other hand, the average apparent activation energy of WHEAT sample assumed values higher than all the other evaluated samples. Actually, it was little higher than those of its components, i.e. Crystal, Trigo and Pilsener malts.

Although comparable E_a values were obtained to that calculated by means of the Kissinger method in previous section, the differences in the activation energy for low and high conversion degrees, indicate that the decomposition process must be evaluated separately. For this reason, the next section deals with the division of the overall process in different stages.

4.3.1.3. Multiple- α analysis for the decomposition in two main stages

While under pyrolysis conditions the degradation of this kind of biomasses gives more clear results and has been studied deeper, the thermal degradation under oxidative conditions is more complex and the results are difficult to ascertain [53]. This is due to the presence of oxidizing agents (oxygen in this case) that contribute to generate simultaneous reactions between oxygen and solid reactants and oxygen and volatiles [53], [54].

As stated before, the initial mass loss from 25 °C to 170-180 °C visible in thermograms, was due to water vaporization (stage 0). Afterwards, two main decomposition stages were found, according to expectations for lignocellulosic biomass [53]. Although this two-stage behavior (stage I and stage II) has been widely reported in the literature, different approaches were proposed for the identification of the components decomposing at each stage. It has been proved that the synergistic and simultaneous purely pyrolytic thermal degradation and heterogeneous oxidation occur during decomposition in oxidative atmosphere, giving as a result a complex thermogram. In this line, the mass loss profile during thermogravimetric analysis may be the sum of the pyrolysis of biomass, the heterogeneous oxidation reactions and the combustion of the generated char. If the biomass composition is considered as a combination of the main components of hemicellulose, cellulose and lignin, the peaks in the DTG curve would be assigned according to the reported stability of these components. However, the reaction mechanism corresponding to the different peaks has been the focus of discussion and two hypotheses have been proposed. The first hypothesis describes that during Stage I, the complete volatilization of the three main constituents of lignocellulosic material (hemicellulose, cellulose and lignin) occurs, followed by the combustion of char residue in Stage II. On the other hand, the second hypothesis considers that, while in the Stage I the hemicellulose and cellulose are completely decomposed, the decomposition of lignin covers a part of stage I, and also of stage II. Therefore, Stage II would involve the conclusion of the decomposition of the lignin together with the decomposition of the char. This second hypothesis has been recently proved by Ding *et al.* and the decomposition of lignin was demonstrated to be a long-lasting process that contributes both in the Stage I and Stage II [52], [53].

In the current work, stage I was identified starting from the temperature of 170-180 °C until to a temperature between 350-415 °C, appropriately selected for every biomass at the different heating rates in a way that the process represented by the peak or double peak in DTG curve was completely concluded. The stage II was considered to start from the end of stage I and continue until the end of the assay, in this case 800 °C. For demonstration purposes, **Figure 4.12** shows the separation in stages of TG and DTG curves for all the malts analyzed at $\beta = 10$ °C/min. Since the curves are dissimilar at the different heating rates, all the boundary temperatures were chosen case by case according to DTG curve.

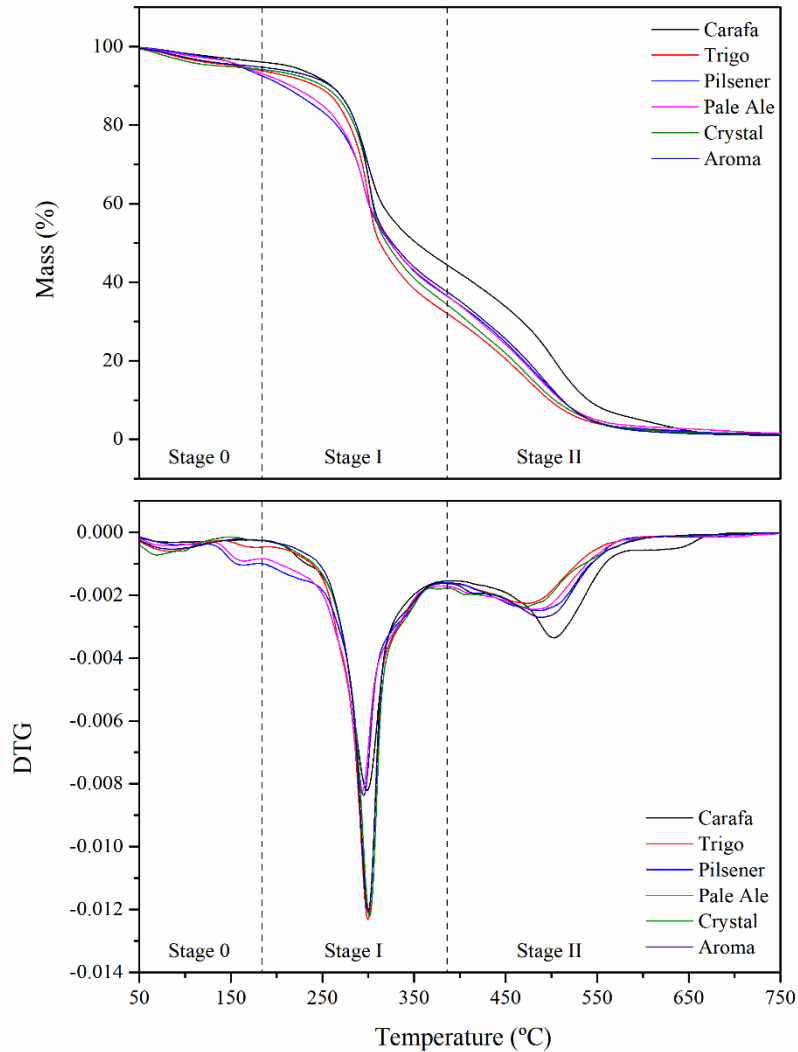


Figure 4.12. Representation of separation in stages for malts at heating rate of 10 °C/min.

Once the processes of malts and BSGs were all separated in the most appropriate way, the same calculations were focused on Stage I and Stage II of all biomasses. In **Figures 4.13, 4.14** and **4.15** are illustrated the linearized plots for both stages of all samples calculated using the Friedman, FWO and KAS methods. All fitting lines show a high degree of correlation. In general, R^2 was always above 0.98 for α in the range 0.2-0.6 while for some biomass, at higher conversion degree it was a little lower but it was always higher than 0.95. From the slopes of the linear fitting of all these plots, the apparent activation energies were calculated at each decomposition degree and plotted in **Figures 4.16, 4.17** and **4.18**.

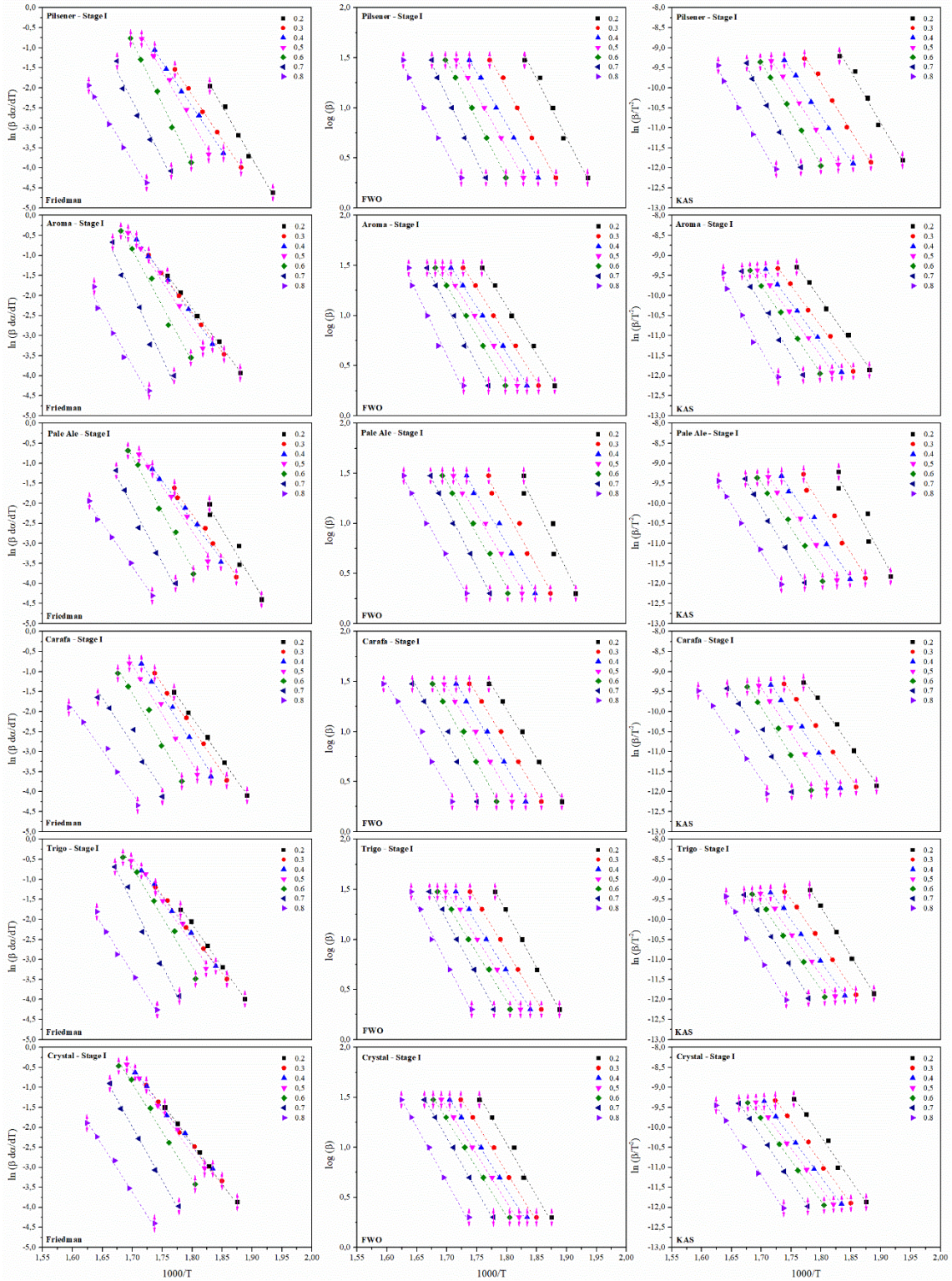


Figure 4.13. Friedman, FWO and KAS fitting plots of malts for stage I at different α .

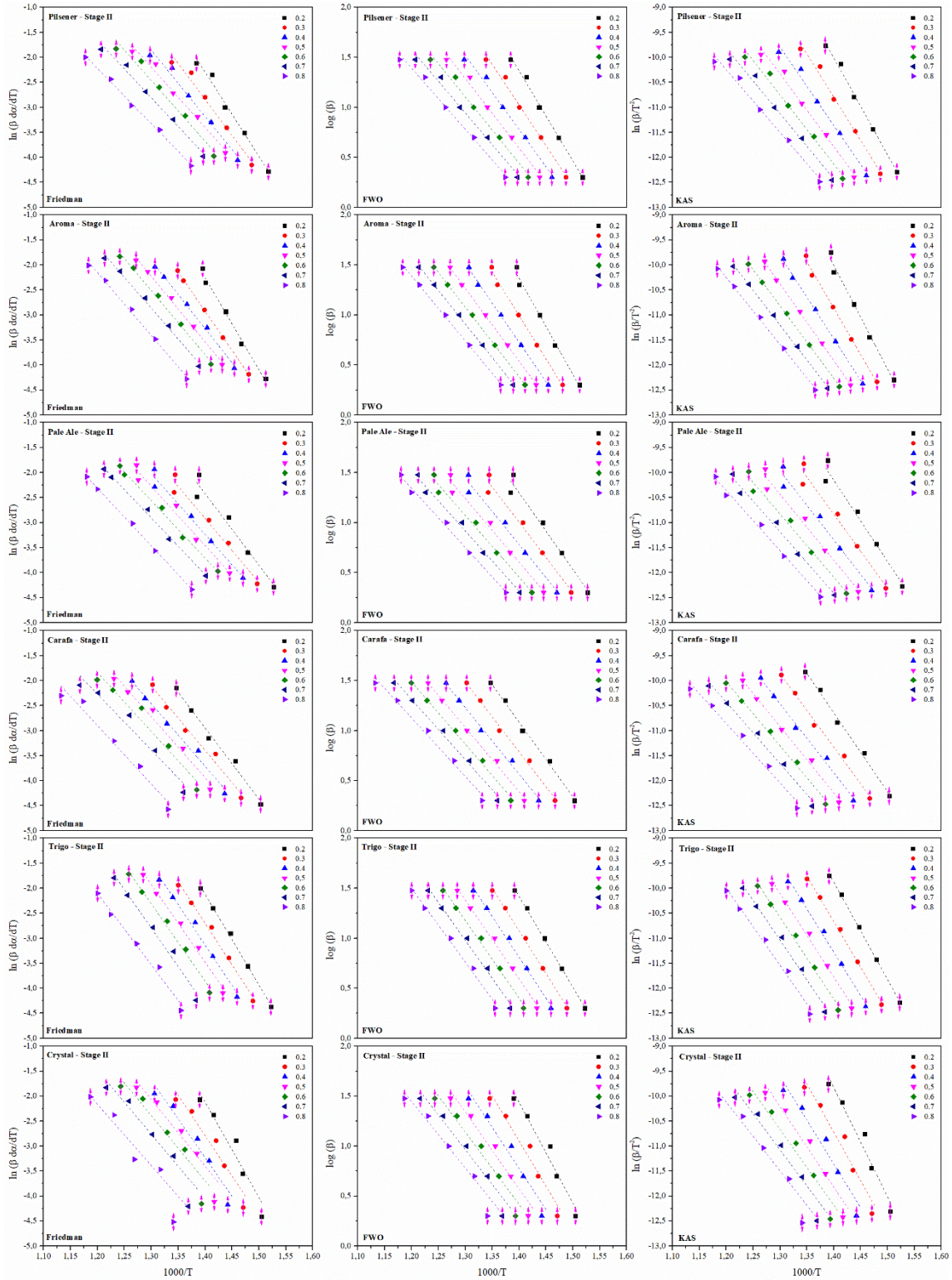


Figure 4.14. Friedman, FWO and KAS fitting plots of malts for stage II at different α .

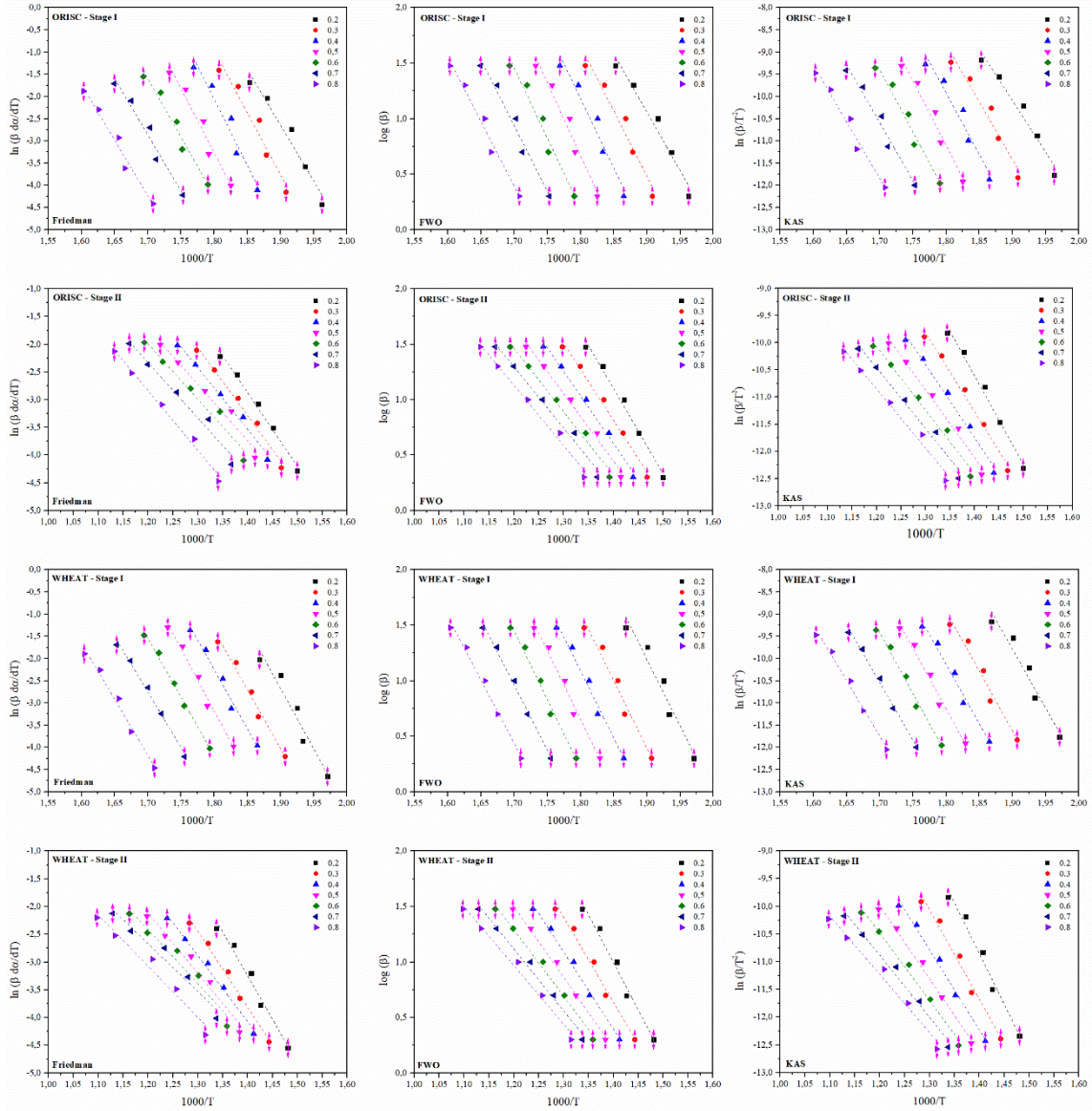


Figure 4.15. Friedman, FWO and FAS fitting plots of ORISC for the two stages at different α .

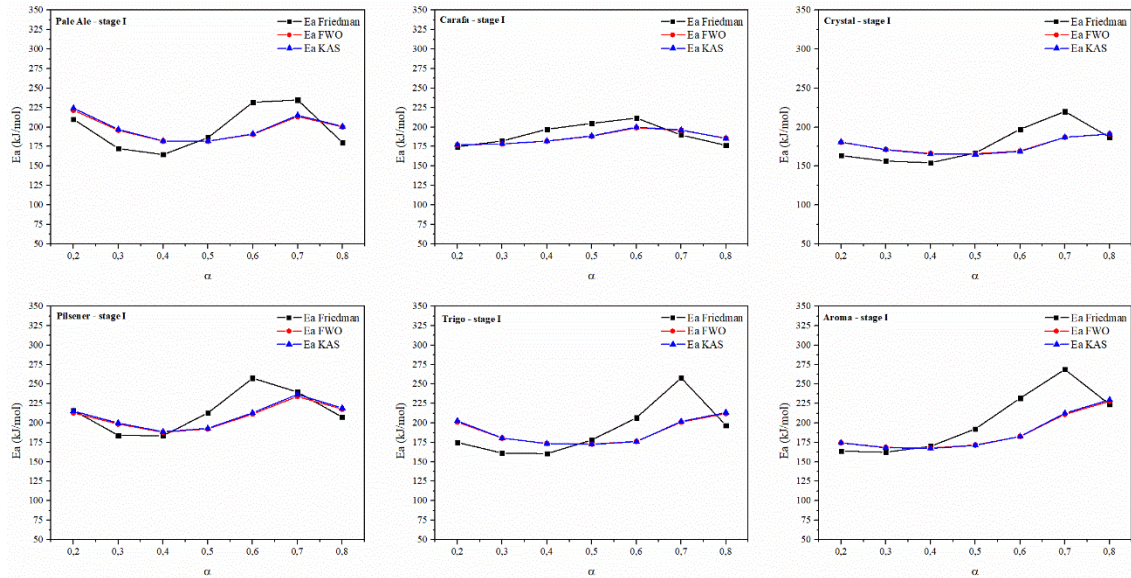


Figure 4.16. Evolution of apparent activation energy of stage I in the range of α 0.2-0.8 calculated with the different iso-conversional methods for all malts.

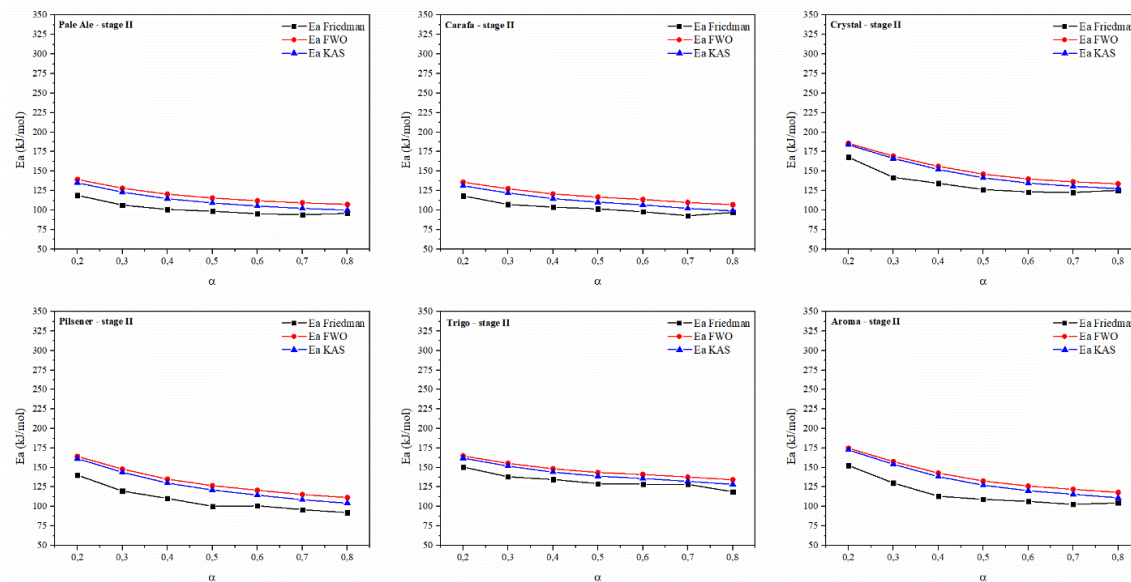


Figure 4.17. Evolution of apparent activation energy of stage II in the range of α 0.2-0.8 calculated with the different iso-conversional methods for all malts.

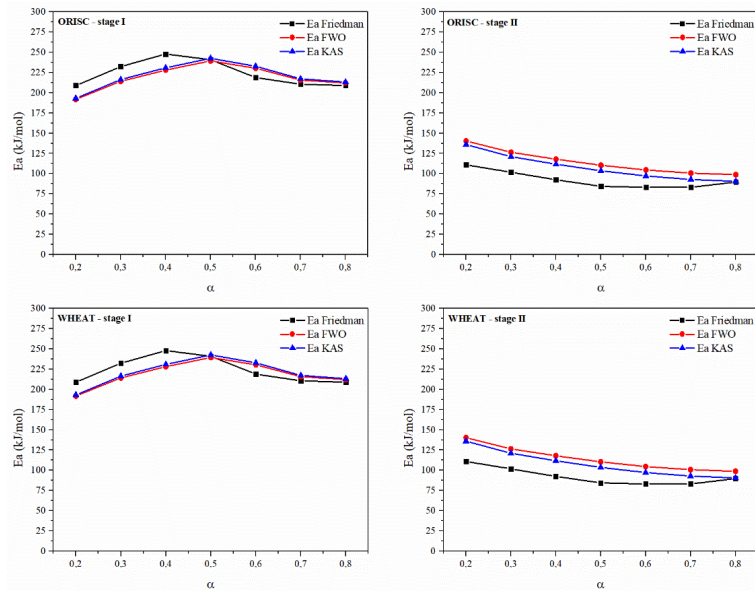


Figure 4.18. Evolution of apparent activation energy of stage I in the range of α 0.2-0.8 calculated with the different iso-conversional methods for ORISC sample.

It is possible to see how in this case the subdivision of overall process into different stages, results in a more constant behaviour of the activation energy in its range of α for most of the analysed samples, with respect to the ones calculated with an overall α for the whole process. This result is more appreciable in the second stage of all samples. This observation can be explained considering the species present in Stage II; remaining fraction of lignin and char products of stage I (hemicellulose char, cellulose char and lignin char). Since these residues are oxidised species, their decomposition behaviour can be considered more homogeneous.

Complementarily, **Table 4.8** gathers the average values for the apparent activation energy calculated in the range of α 0.2-0.8. These averaged values were in line with other studies focused on different types of lignocellulosic biomasses, in which activation energy are always in the range 140-200 kJ/mol considering the same spectrum of α [55], [56].

Table 4.8. Average values for the apparent activation energy (E_a) obtained with the different iso-conversional methods for both Stage I and Stage II.

	Stage I			Stage II		
	E_{aFWO} (kJ·mol ⁻¹)	E_{aKAS} (kJ·mol ⁻¹)	$E_{aFriedman}$ (kJ·mol ⁻¹)	E_{aFWO} (kJ·mol ⁻¹)	E_{aKAS} (kJ·mol ⁻¹)	$E_{aFriedman}$ (kJ·mol ⁻¹)
Carafa	187 ± 7	187 ± 7	191 ± 12	119 ± 8	112 ± 9	103 ± 6
Aroma	186 ± 19	187 ± 20	202 ± 34	139 ± 17	134 ± 18	117 ± 14
Crystal	176 ± 9	176 ± 9	178 ± 20	153 ± 15	148 ± 17	135 ± 12
Pale Ale	198 ± 12	199 ± 12	197 ± 24	119 ± 9	113 ± 10	102 ± 6
Trigo	188 ± 14	189 ± 15	191 ± 25	147 ± 8	142 ± 9	133 ± 7
Pilsener	208 ± 13	210 ± 13	215 ± 20	132 ± 15	126 ± 16	109 ± 13
ORISC	219 ± 12	221 ± 12	224 ± 14	114 ± 12	108 ± 13	92 ± 8
WHEAT	219 ± 5	221 ± 5	220 ± 7	121 ± 17	114 ± 19	95 ± 17

As expected, the activation energy of Stage I is significantly higher than that of Stage II. Particularly, an average of 190-200 kJ/mol was found. Looking at the results of the six malts, the only significant difference is the Crystal malts, which has a lower E_a in Stage I and also the activation energy for the Stage II does not decrease as considerably as other malts. The result could have been anticipated even looking at the variation of activation energy in the previous section, when an overall perspective was considered (**Figure 4.9**) and the activation energy was almost constant in the entire range of conversion.

Looking at the activation energies of the two BSGs samples, non-significant variations were noted between them. They performed quite similar for both stages and, in general, the values in Stage I were higher than the single mashed malts of which they are composed while were lower in Stage II. The interaction of different simultaneous thermo-chemical decomposition reactions of the different malt varieties composing ORISC and WHEAT may have increased the activation energy of the entire Stage I.

In general, the apparent activation energies calculated separating the stages were steadier (lower deviation) with respect to those calculated with an overall approach. Considering that the mass loss was higher in Stage I, the average values between the two stages that can be obtained here, reflect the average values calculated in previous section, with an overall α . However, the values calculated in this way can be considered more appropriate because better reflect the real behaviour of this kind of biomasses when subjected to thermo-oxidative decomposition thus, degradation stage by stage.

The values of apparent activation energy showed in **Table 4.8** are always fairly similar for FWO and KAS methods, while are a little different for Friedman method that also present, in most of the cases, the higher deviation from the mean. This could be due to the differential nature of this method that, after the required numerical differentiation, could give this slightly diverse result [48].

Making use of these calculated values of the apparent activation energy, in the next section the kinetic function and the pre-exponential factor of each analysed sample will be calculated.

4.3.2. Calculation of kinetic function and pre-exponential factor

In order to complete the kinetic triplet, the mechanism of reaction and the pre-exponential factor should be calculated. The most appropriate mechanism for each sample in the two stage was graphically evaluated using reduced Master Plots. In the **Figures 4.19, 4.20** and **4.21** are illustrated the experimental curves at heating rate of 10 °C/min in comparison to some of the theoretical $g(\alpha)$ curves for the typical decomposition mechanisms of biomass, gathered in **Table 3.4**.

Looking at the comparison between master curves and experimental curves of malts and spent grains, it was possible to see that all the reaction mechanisms for Stage I were comparable to curve F_n type, with n equal to 2, 3, 4 and 5. Physically speaking, F mechanisms represent solid state processes in which random nucleation with one, two or three nuclei on the individual particle takes place.

However, Stage II revealed a mechanism more difficult to assign. Although experimental curves were always between F_n and D_n models, the mechanism selected as the most appropriate to describe all the experimental results of Stage II was the D_4 type, which $f(\alpha)$ and $g(\alpha)$ equations are presented in **Table 3.4**. This mechanism describes a solid-state process in which three-dimensional diffusion occur.

These mechanisms are in accordance with results reported in literature, in which the mechanism of decomposition of lignocellulosic materials under oxidative conditions for temperatures in the range of those selected for Stage I (mostly attributed to hemicellulose and cellulose) is often identified as a F mechanism, while decomposition of Stage II (attributed to remaining lignin and char) is sometimes described according to F_n , A_n or D_n mechanism, but it may change for different materials [9], [48], [49].

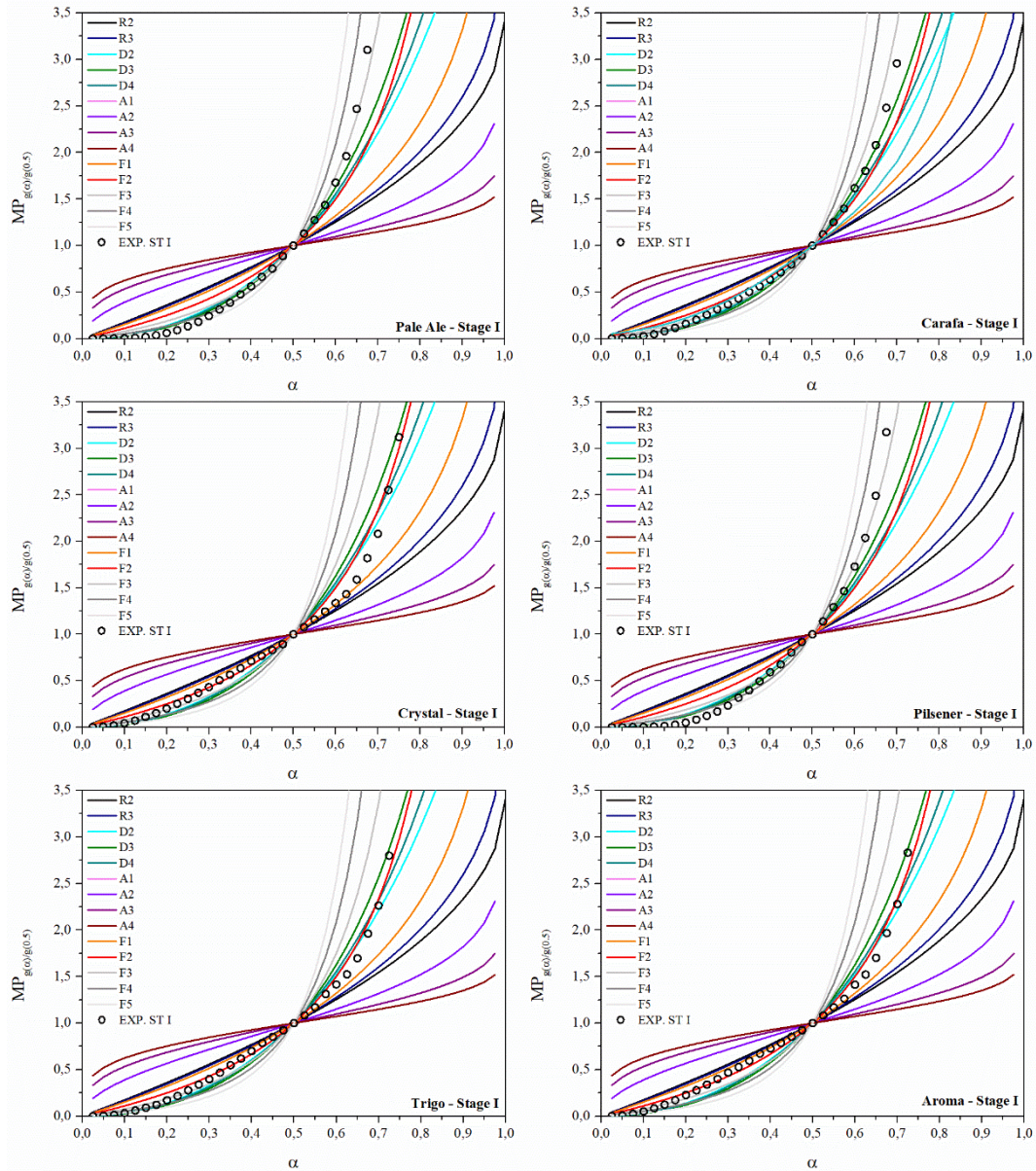


Figure 4.19. Normalised Master Plots in comparison to the Stage I decomposition process of all the malt samples at a heating rate of 10 °C/min.

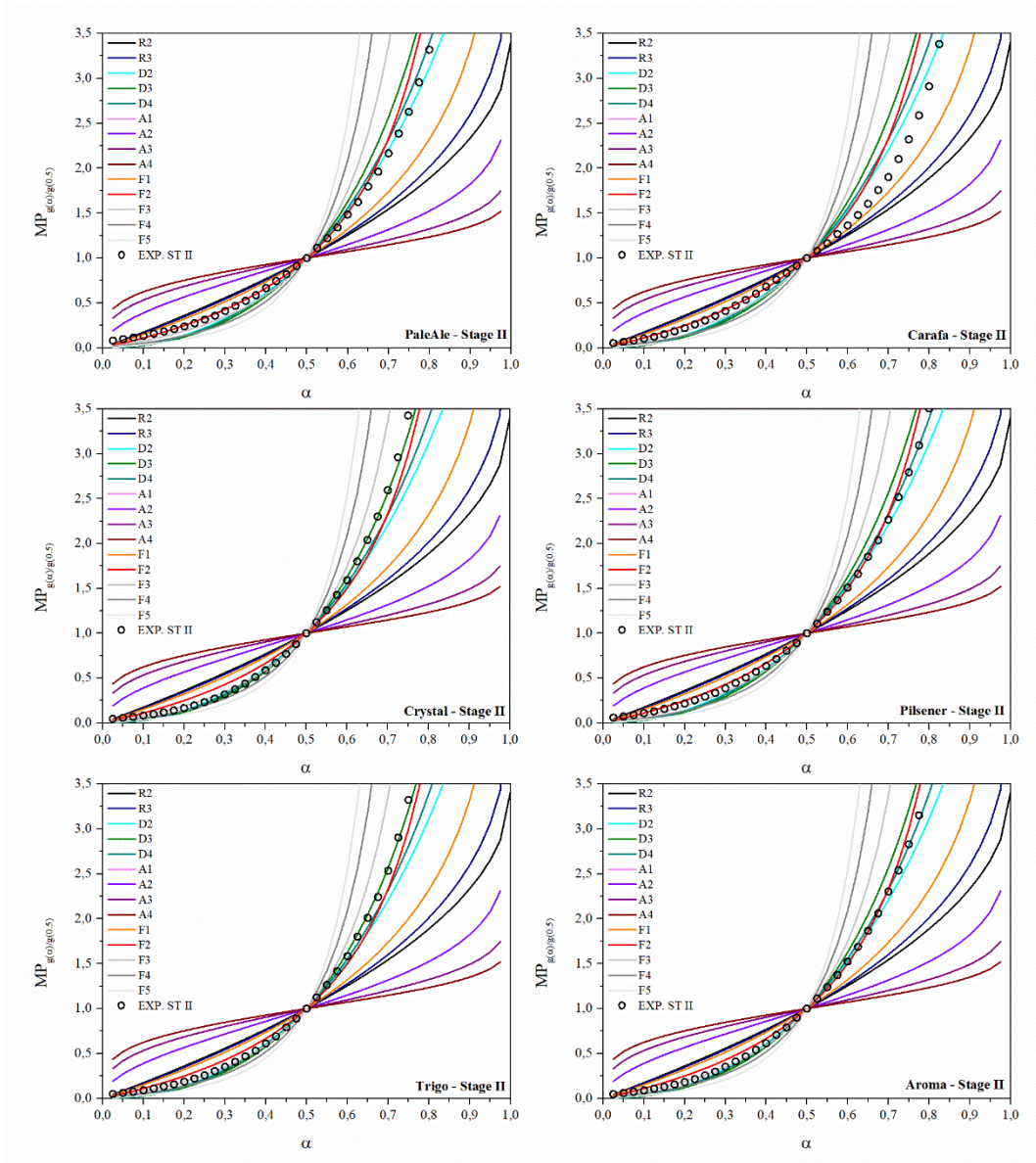


Figure 4.20. Normalised Master Plots in comparison to the Stage II decomposition process of all the malt samples at a heating rate of 10 °C/min.

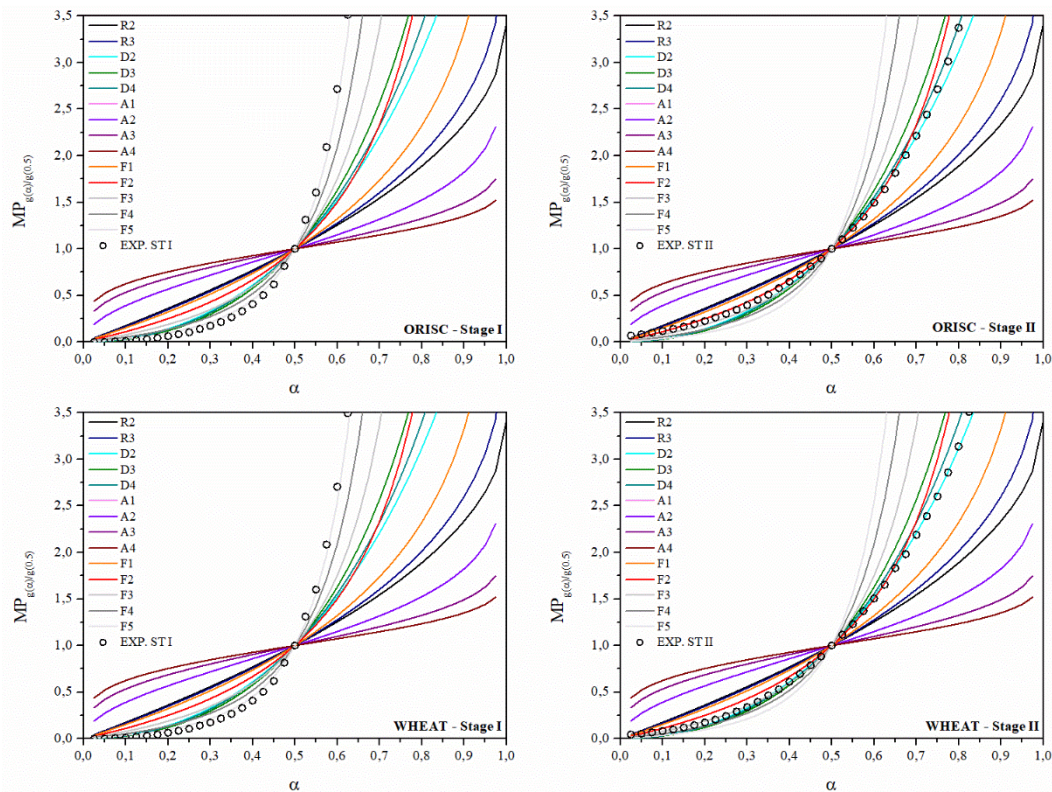


Figure 4.21. Normalised Master Plots in comparison to the Stage I and Stage II decomposition process of the BSGs (ORISC and WHEAT) at a heating rate of 10 °C/min.

Once the best theoretical mechanism was graphically evaluated, applying the Coast-Redfern equation (equation (3.17)), the pre-exponential factor A and the optimal analytical n were evaluated for the selected mechanism. Using the average value of activation energies calculated with the three iso-conversional methods and applying a regression method the value of n was calculated.

Subsequently, $\ln A$ was calculated from the intercept with the axis of the line of plots $\ln \left(\beta \frac{g(\alpha)}{T^2} \right)$ vs $\frac{1}{T}$ for each heating rate. According to Perez-Maqueda criterion, the points should lie on the same straight line if the appropriate $g(\alpha)$ is chosen. In **Figure 4.22** and **Figure 4.23** are illustrated these behaviours for malts in Stage I and Stage II, respectively. As well, **Figure 4.24** shows the curves for Stage I and Stage II of ORISC and WHEAT brewer's spent grains.

The validity of the simplified kinetic triplet was also assessed, being its use advisable when the activation energy could be considered constant within a narrow confidence interval [57]. Moreover, the straight lines in the Perez-Maqueda criterion figures confirm the good fitting of selected mechanisms (F_n and D_4).

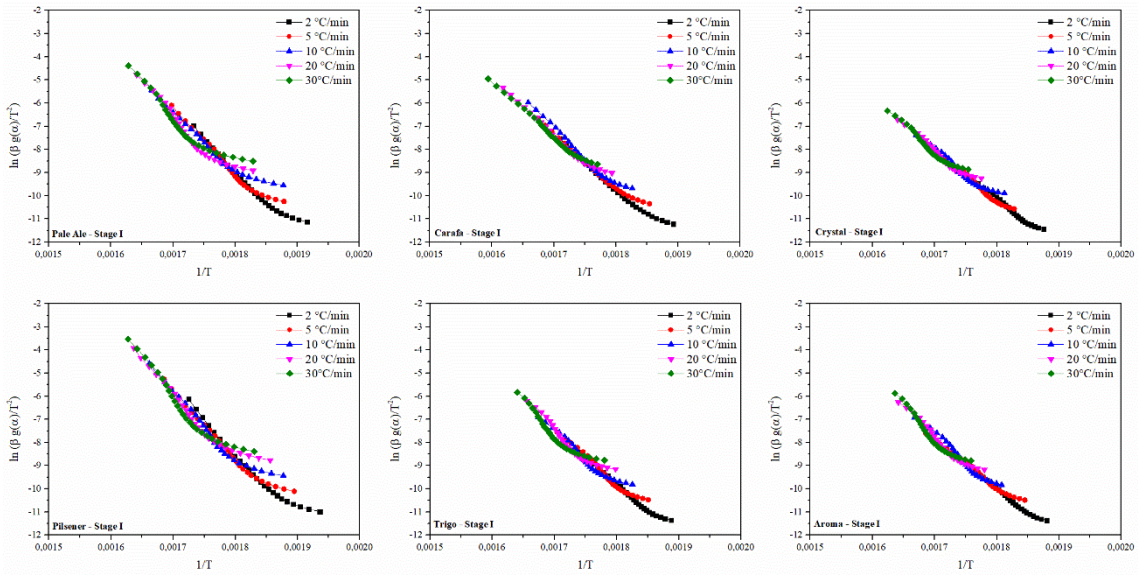


Figure 4.22. Application of the Perez-Maqueda et al. criterion for the simplified kinetic triplet of stage I of malts at heating rate equal to 2, 5, 10, 20, 30 °C/min.

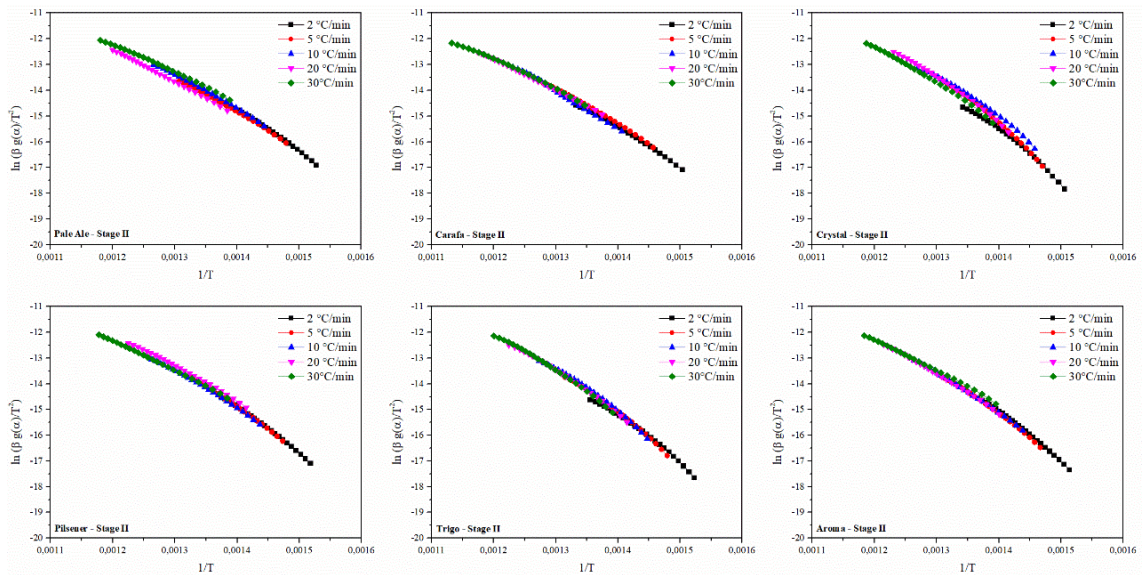


Figure 4.23. Application of the Perez-Maqueda et al. criterion for the simplified kinetic triplet of stage II of malts at heating rate equal to 2, 5, 10, 20, 30 °C/min.

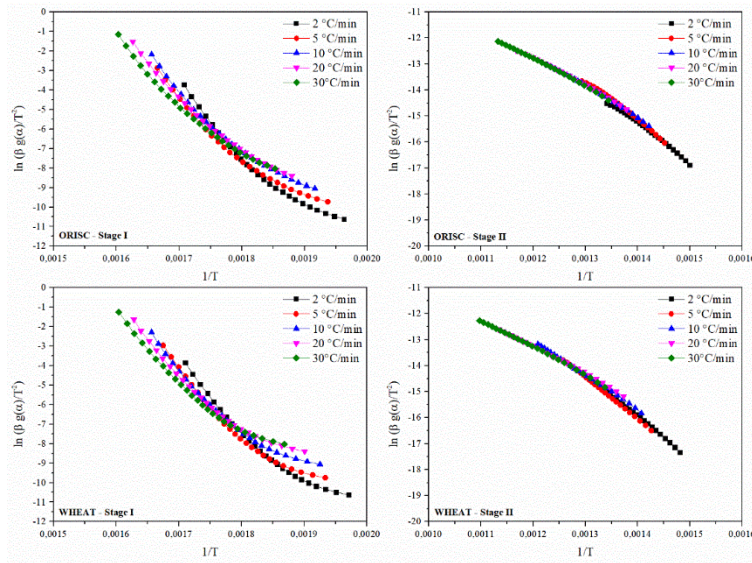


Figure 4.24. Application of the Perez-Maqueda et al. criterion for the simplified kinetic triplet of stage I and stage II of ORISC and WHEAT at heating rate equal to 2, 5, 10, 20, 30 °C/min.

Since the passages from Stage 0 to Stage I and, from Stage I to Stage II, are not always obvious, the small deviation from linearity noticeable at the edges, mostly at low temperatures of Stage I of Pilsener, Pale Ale and both BSGs, is explainable by the fact that at these temperatures some trace of remnant water was still present at the beginning of this stage.

In **Table 4.9** are illustrated the values of pre-exponential factor calculated as an average between the A_{β} at the different heating rates, the most appropriate mechanism of reaction and the calculated analytical order for all malts, ORISC and WHEAT BSGs, in Stage I and Stage II. Moreover, e (%) represents the average of absolute deviations from the mean in each set of $\ln A_{\beta}$.

Table 4.9. Frequency factor A, reaction mechanism and reaction analytical order calculated applying Perez-Maqueda criterion for malts and BSGs on both stages.

	Stage I				Stage II			
	$\ln(A)$	e (%)	n -MP	n	$\ln(A)$	e (%)	n -MP	n
Carafa	40.0	6	F3	2.8	13.0	17	D4	-
Aroma	41.8	12	F2-F3	2.2	16.4	21	D4	-
Crystal	38.1	5	F2	1.9	19.1	18	D4	-
Pale Ale	40.9	7	F3	3.1	13.4	17	D4	-
Trigo	39.5	4	F2-F3	2.2	18.9	10	D4	-
Pilsener	45.6	5	F3-F4	3.7	15.3	21	D4	-
ORISC	47.7	4	F5	5.2	12.4	24	D4	-
WHEAT	47.6	3	F5	5.1	12.4	26	D4	-

The obtained results are quite similar for all considered malts in the two stages, both in terms of pre-exponential factor and kinetic function. On the other hand, the two BSGs, ORISC and WHEAT, showed almost identical results. However, if compared malts and BSGs, the results obtained in this work revealed slightly different pattern. In this regard, some differences could be identified between the BSGs and the malts by which they were supposed to be composed.















4.4. Pelletised BSGs as combustion fuel

Given the minor perceived differences in terms of thermo-oxidative decomposition among the different malt varieties, the BSGs were all pelletised together. Subsequently, for validation purposes, the pellets were preliminarily subjected to combustion in a muffle furnace at different temperatures ranging from 400 to 700 °C. These temperatures were selected according to the results found in the thermo-oxidative stability analyses, which revealed complete combustion from about 500 °C onwards. Temperatures below 500 °C were selected for monitoring purposes. After combustion, the ash yields were calculated and their appearance was evaluated, both gathered in **Table 4.10**.

In general, ash yields below 3.5% for combustion above 450 °C were found, which slightly decreased with higher temperatures up to 2.4% at 700 °C. The ash percentage was comparable to that found for the combustion of the grounded BSGs measured according to normalised conditions. However, the experiments carried out at 400 °C revealed partial combustion, with a 7.0% of residue. As a whole, the shape of the pellets remained unaltered after combustion, but powder was obtained after slight agitation of the tray, especially at temperatures higher than 500 °C. It must be highlighted that the combustion at temperatures below 500 °C resulted in the generation of more carbonaceous ash, given the blackish colour of the powder and more consistent morphology. On the other hand, above 500 °C, pure ash with a greyish colour was obtained, typical for the complete combustion of biomass. In this line, the combustion of BSGs in gasification processes at temperatures above 500 °C would allow for the lowest ash yield and a powder morphology, manageable in automated setups [58] and useful for a variety of further applications [59].

This hypothesis was validated in an incineration pilot plant, in which 1 kg of BSG pellets was applied. A pellet feeding rate of about 1 kg/h and airflow of 50 L/min (21% O₂) were considered to ensure that combustion was accomplished at temperatures above 500 °C. Although flames in these experimental tests experience large temporal and spatial gradients in local species and temperatures, they remained virtually constant during the whole operation, as observed through the viewing port and shown in **Figure 4.25** [60].

Table 4.10. Ash percentage and appearance of the pellets after combustion at different temperatures.

Temperature (°C)	Ash (%)	Appearance before agitation	Appearance after agitation
400	7.05		
450	3.33		
500	3.39		
550	2.52		
600	2.64		
650	2.51		
700	2.44		

Once the pellets were consumed, the incineration unit was opened, and the remnant ash in the combustion chamber was collected into the ashtray in the bottom, as shown in **Figure 4.25**. The combustion ash revealed a greyish powder appearance, as found after muffle furnace combustion assays. Given the contribution of the moving grill in a circular motion of the incineration unit, powder together with particles lower than 1.5 mm was obtained, as can be observed in **Figure 4.25**. For the considered amount of 1 kg of pellets, 24.12 g of ash were gained, which represent a yield of 2.4%. This result is in accordance with that found in the muffle furnace experiments at temperatures above 500 °C, and also with that determined in the proximate analysis. Moreover, given its powder morphology, the ash revealed an apparent density of 0.37 g/mL. Therefore, the reliable combustion behaviour, along with the higher heating value of about 18 MJ/kg found in previous sections, makes this biomass a potential candidate for being used as a source of energy in combustion incineration devices. Although ash was not adhered in the walls of the incineration unit and could be properly managed, further characterisation of ash would allow for a deeper evaluation in terms of ash formation and deposition mechanisms, particle properties or sticking behaviour [61].



Figure 4.25. Flame during combustion (left), residue into the incineration unit after combustion (middle), and collected ash (right).

5. CONCLUSIONS

An accurate methodology was developed to valorise the wastes of two beer spent grains (BSGs) produced in a pilot-scale brewery and their constituent malts, to use them as feedstock to produce energy.

Both beer spent grains (BSGs) and malts are mainly composed of Carbon and Oxygen, have a low Nitrogen and a null Sulphur content. These chemical properties make these materials attractive during combustion providing a major environmental advantage instead of fossil fuels. With an exhaustive control of the combustion temperature, the products will mainly be carbon dioxide and monoxide, while the production of unwanted nitrogenous compounds will be in lower proportions.

Both beer spent grains (BSGs) and the different malt varieties have similar values of volatiles proportion, and the ash yield is low. Only the BSGs types with raw Carafa malt in their composition have a slightly higher ash yield but are low enough to avoid operational difficulties.

The higher heating value (*HHV*) is practically equal for both types of BSGs. These results suggest the possibility of using various BSGs mixed without producing a significant decrease in the calorific values.

Both beer spent grains (BSGs) and the different malt varieties exhibited three degradation stages corresponding to the main components: (i) a devolatilization of residual humidity (Stage 0); (ii) the thermo-oxidation of hemicellulose, cellulose, and partially lignin (Stage I); and (iii) the thermo-oxidation of and remnant lignin and char (Stage II). The thermal stability, the zero-decomposition temperature, and volatile peak temperatures are quite similar but differ in the thermo-oxidation range due to the interaction between the components.

The kinetic triplet, involving activation energies, pre-exponential factor values, and mechanisms of the reactions evaluated predict the devolatilization in thermo-oxidative conditions and are the input variables in a theoretical model to describe the thermal recovery processes in a reactor using these biomasses as feedstock. Stage I of malts and BSGs was always described by random nucleation kinetic model (*FFnn*) and the activation energy of BSGs was higher than their respective single mashed malts. Stage II was described by a three-dimensional diffusion kinetic model (*DD4*), similar to other lignocellulosic materials. The activation energy of this stage for BSGs is lower than their respective single mashed malts.

Finally, pelletised BSGs subjected to combustion processes in a pilot incineration plant verified the low ash formation with a fine powder morphology, especially when combustion was carried out above 500 °C.



UNIVERSITAT
POLITÈCNICA
DE VALÈNCIA



ESCOLA TÈCNICA
SUPERIOR ENGINYERIA
INDUSTRIAL VALÈNCIA

Bibliography

- [1] J. S. Lim, Z. Abdul Manan, S. R. Wan Alwi, and H. Hashim, "A review on utilisation of biomass from rice industry as a source of renewable energy," *Renew. Sustain. Energy Rev.*, vol. 16, no. 5, pp. 3084–3094, 2012, doi: 10.1016/j.rser.2012.02.051.
- [2] "statistic_id270275_global-beer-production-1998-2019.pdf."
- [3] Y. Shen *et al.*, "Feed nutritional value of brewers' spent grain residue resulting from protease aided protein removal," *J. Anim. Sci. Biotechnol.*, vol. 10, no. 1, pp. 1–10, 2019, doi: 10.1186/s40104-019-0382-1.
- [4] P. Tanger, J. L. Field, C. E. Jahn, M. W. DeFoort, and J. E. Leach, "Biomass for thermochemical conversion: Targets and challenges," *Frontiers in Plant Science*, vol. 4, no. JUL. Frontiers Research Foundation, Jul. 01, 2013, doi: 10.3389/fpls.2013.00218.
- [5] N. Epstein and J. R. Grace, *Spouted and spout-fluid beds : fundamentals and applications*. Cambridge University Press, 2011.
- [6] P. McKendry, "Energy production from biomass (part 1): Overview of biomass," *Bioresour. Technol.*, vol. 83, no. 1, pp. 37–46, 2002, doi: 10.1016/S0960-8524(01)00118-3.
- [7] J. E. White, W. J. Catallo, and B. L. Legendre, "Biomass pyrolysis kinetics: A comparative critical review with relevant agricultural residue case studies," *J. Anal. Appl. Pyrolysis*, vol. 91, no. 1, pp. 1–33, 2011, doi: 10.1016/j.jaap.2011.01.004.
- [8] S. Y. Yorulmaz and A. T. Atimtay, "Investigation of combustion kinetics of treated and untreated waste wood samples with thermogravimetric analysis," *Fuel Process. Technol.*, vol. 90, no. 7–8, pp. 939–946, 2009, doi: 10.1016/j.fuproc.2009.02.010.
- [9] D. López-González, M. Fernandez-Lopez, J. L. Valverde, and L. Sanchez-Silva, "Thermogravimetric-mass spectrometric analysis on combustion of lignocellulosic biomass," *Bioresour. Technol.*, vol. 143, pp. 562–574, 2013, doi: 10.1016/j.biortech.2013.06.052.
- [10] M. Li, L. Jiang, J. J. He, and J. H. Sun, "Kinetic triplet determination and modified mechanism function construction for thermo-oxidative degradation of waste polyurethane foam using conventional methods and distributed activation energy model method," *Energy*, vol. 175, pp. 1–13, 2019, doi: 10.1016/j.energy.2019.03.032.
- [11] S. Yakoyama and M. Yukihiro, "The Asian Biomass Handbook Support Project for Building Asian-Partnership for," *Japan Inst. Energy*, p. 338, 2008.
- [12] H. of C. E. A. Committee, "Are biofuels sustainable," *Gov. Response*, vol. I, no. January, 2008, [Online]. Available: <http://scholar.google.com/scholar?hl=en&btnG=Search&q=intitle:Are+biofuels+sustainable+#3%0Ahttp://www.publications.parliament.uk/pa/cm200708/cmselect/cmenvaud/cmenvaud.htm>.
- [13] S. Yaman, "Pyrolysis of biomass to produce fuels and chemical feedstocks," *Energy Convers. Manag.*, vol. 45, no. 5, pp. 651–671, 2004, doi: 10.1016/S0196-8904(03)00177-8.
- [14] Davis, S.C., Hay, Pierce, W., and J., *Biomass in the energy industry : An introduction*. 2014.
- [15] I. Cunningham and G. Dawes, "Background and introduction," *Self Manag. Learn. Action Putt. SML into Pract.*, pp. 5–18, 2017, doi: 10.4324/9780203469514_chapter_1.
- [16] International Renewable Energy Agency (IRENA), "Renewable Capacity 2019," no. March, p. 3,

- 2019, [Online]. Available: www.irena.org/publications.
- [17] B. Sorensen, "Renewable Energy," *Renew. Energy*, 2011, doi: 10.1016/C2009-0-30432-8.
- [18] C. J. Gómez and C. J. Gomez Diaz, "Understanding Biomass Pyrolysis Kinetics : Improved Modeling Based on Comprehensive Thermokinetic Analysis," *Univ. Politec. Catalunya*, p. 106, 2006.
- [19] N. C. for D. C. (NCDC), "2020 Edition," *Natl. Guidel. Infect. Prev. Control Viral Hemorrhagic Fevers*, no. January, p. 112, 2020, [Online]. Available: https://ncdc.gov.ng/themes/common/docs/protocols/111_1579986179.pdf.
- [20] K. Kundu, A. Chatterjee, T. Bhattacharyya, M. Roy, and A. Kaur, *Thermochemical Conversion of Biomass to Bioenergy: A Review*, no. January. 2018.
- [21] P. Bajpai, *Biomass conversion processes*. 2020.
- [22] W. I. Biomass, "Biomass Use of Biomass," pp. 10–14, 2018.
- [23] L. Directive, L. Directive, and L. Directive, "Landfill Gas Control -Guidance on the landfill gas control requirements of the Landfill Directive," pp. 1–7.
- [24] F. Wikipedia, "Ethanol fuel in the United States," pp. 1–24, 2012.
- [25] R. dos S. M. Thiago, P. M. de M. Pedro, and F. C. S. Eliana, "Solid wastes in brewing process: A review," *J. Brew. Distill.*, vol. 5, no. 1, pp. 1–9, 2014, doi: 10.5897/jbd2014.0043.
- [26] S. I. Mussatto, G. Dragone, and I. C. Roberto, "Brewers' spent grain: Generation, characteristics and potential applications," *J. Cereal Sci.*, vol. 43, no. 1, pp. 1–14, 2006, doi: 10.1016/j.jcs.2005.06.001.
- [27] D. S. Tang *et al.*, "Recovery of protein from brewer's spent grain by ultrafiltration," *Biochem. Eng. J.*, vol. 48, no. 1, pp. 1–5, 2009, doi: 10.1016/j.bej.2009.05.019.
- [28] M. Ribau Teixeira, E. C. Guarda, E. B. Freitas, C. F. Galinha, A. F. Duque, and M. A. M. Reis, "Valorization of raw brewers' spent grain through the production of volatile fatty acids," *N. Biotechnol.*, vol. 57, no. August 2019, pp. 4–10, 2020, doi: 10.1016/j.nbt.2020.01.007.
- [29] S. T. Cooray and W. N. Chen, "Valorization of brewer's spent grain using fungi solid-state fermentation to enhance nutritional value," *J. Funct. Foods*, vol. 42, no. October 2017, pp. 85–94, 2018, doi: 10.1016/j.jff.2017.12.027.
- [30] P. Klímek, R. Wimmer, P. Kumar Mishra, and J. Kúdela, "Utilizing brewer's-spent-grain in wood-based particleboard manufacturing," *J. Clean. Prod.*, vol. 141, no. February, pp. 812–817, 2017, doi: 10.1016/j.jclepro.2016.09.152.
- [31] W. Russ, H. Mörtel, R. Meyer-Pittroff, and A. Babeck, "Kieselguhr sludge from the deep bed filtration of beverages as a source for silicon in the production of calcium silicate bricks," *J. Eur. Ceram. Soc.*, vol. 26, no. 13, pp. 2547–2559, 2006, doi: 10.1016/j.jeurceramsoc.2005.04.023.
- [32] International Organization for Standardization, "UNE-EN ISO 18122:2016 Solid biofuels. Determination of ash content.," 2016.
- [33] International Organization for Standardization, "UNE-EN ISO 18123:2016 Solid biofuels. Determination of the content of volatile matter.," 2016.
- [34] International Organization for Standardization, "UNE-EN ISO 18134-1:2016 Solid biofuels. Determination of moisture content - Oven dry method - Part 1: Total moisture - Reference method.," 2016.

- [35] S. A. Channiwala and P. P. Parikh, "A unified correlation for estimating HHV of solid, liquid and gaseous fuels," *Fuel*, vol. 81, no. 8, pp. 1051–1063, 2002, doi: 10.1016/S0016-2361(01)00131-4.
- [36] T. Lever, P. Haines, J. Rouquerol, E. L. Charsley, P. Van Eckeren, and D. J. Burlett, "ICTAC nomenclature of thermal analysis (IUPAC Recommendations 2014)," *Pure Appl. Chem.*, vol. 86, no. 4, pp. 545–553, 2014, doi: 10.1515/pac-2012-0609.
- [37] T. Hirata and K. E. Werner, "Thermal analysis of cellulose treated with boric acid or ammonium phosphate in varied oxygen atmospheres," *J. Appl. Polym. Sci.*, vol. 33, pp. 1533–1556, 1987.
- [38] A. Khawam and D. R. Flanagan, "Solid-state kinetic models: basics and mathematical fundamentals," *J. Phys. Chem. B*, vol. 110, no. 35, pp. 17315–17328, Sep. 2006, doi: 10.1021/jp062746a.
- [39] H. E. Kissinger, "Reaction Kinetics in Differential Thermal Analysis," *Anal. Chem.*, vol. 29, no. 11, pp. 1702–1706, 1957, doi: 10.1021/ac60131a045.
- [40] J. D. Badia, L. Santonja-Blasco, A. Martínez-Felipe, and A. Ribes-Greus, "A methodology to assess the energetic valorization of bio-based polymers from the packaging industry: Pyrolysis of reprocessed polylactide," *Bioresour. Technol.*, vol. 111, pp. 468–475, 2012, doi: 10.1016/j.biortech.2012.02.013.
- [41] J. H. Flynn and L. A. Wall, "A quick, direct method for the determination of activation energy from thermogravimetric data," *J. Polym. Sci. Part B Polym. Lett.*, vol. 4, no. 5, pp. 323–328, 1966, doi: <https://doi.org/10.1002/pol.1966.110040504>.
- [42] T. Ozawa, "A New Method of Analyzing Thermogravimetric Data," *Bull. Chem. Soc. Jpn.*, vol. 38, no. 11, pp. 1881–1886, 1965, doi: 10.1246/bcsj.38.1881.
- [43] H. L. Friedman, "Kinetics of thermal degradation of char-forming plastics from thermogravimetry. Application to a phenolic plastic," *J. Polym. Sci. Part C Polym. Symp.*, vol. 6, no. 1, pp. 183–195, 1964, doi: <https://doi.org/10.1002/polc.5070060121>.
- [44] J. M. Criado, J. Málek, and A. Ortega, "Applicability of the master plots in kinetic analysis of non-isothermal data," *Thermochim. Acta*, vol. 147, no. 2, pp. 377–385, Jul. 1989, doi: 10.1016/0040-6031(89)85192-5.
- [45] L. A. Pérez-Maqueda and J. M. Criado, "Accuracy of Senum and Yang's approximations to the Arrhenius integral," *J. Therm. Anal. Calorim.*, vol. 60, no. 3, pp. 909–915, 2000, doi: 10.1023/A:1010115926340.
- [46] L. A. Pérez-Maqueda, J. M. Criado, F. J. Gotor, and J. Málek, "Advantages of combined kinetic analysis of experimental data obtained under any heating profile," *J. Phys. Chem. A*, vol. 106, no. 12, pp. 2862–2868, 2002, doi: 10.1021/jp012246b.
- [47] A. W. COATS and J. P. REDFERN, "Kinetic Parameters from Thermogravimetric Data," *Nature*, vol. 201, no. 4914, pp. 68–69, 1964, doi: 10.1038/201068a0.
- [48] C. Moliner, B. Bosio, E. Arato, and A. Ribes, "Thermal and thermo-oxidative characterisation of rice straw for its use in energy valorisation processes," *Fuel*, vol. 180, pp. 71–79, 2016, doi: 10.1016/j.fuel.2016.04.021.
- [49] C. Moliner, K. Aguilar, B. Bosio, E. Arato, and A. Ribes, "Thermo-oxidative characterisation of the residues from persimmon harvest for its use in energy recovery processes," *Fuel Process. Technol.*, vol. 152, pp. 421–429, 2016, doi: 10.1016/j.fuproc.2016.07.008.
- [50] A. Chetrariu and A. Dabija, "Brewer's spent grains: Possibilities of valorization, a review," *Appl.*

Sci., vol. 10, no. 16, pp. 1–17, 2020, doi: 10.3390/app10165619.

- [51] M. Jackowski *et al.*, “HTC of wet residues of the brewing process: Comprehensive characterization of produced beer, spent grain and valorized residues,” *Energies*, vol. 13, no. 8, 2020, doi: 10.3390/en13082058.
- [52] D. K. Shen, S. Gu, K. H. Luo, A. V. Bridgwater, and M. X. Fang, “Kinetic study on thermal decomposition of woods in oxidative environment,” *Fuel*, vol. 88, no. 6, pp. 1024–1030, 2009, doi: 10.1016/j.fuel.2008.10.034.
- [53] Y. Ding, B. Huang, C. Wu, Q. He, and K. Lu, “Kinetic model and parameters study of lignocellulosic biomass oxidative pyrolysis,” *Energy*, vol. 181, pp. 11–17, 2019, doi: 10.1016/j.energy.2019.05.148.
- [54] M. V. Gil, D. Casal, C. Pevida, J. J. Pis, and F. Rubiera, “Thermal behaviour and kinetics of coal/biomass blends during co-combustion,” *Bioresour. Technol.*, vol. 101, no. 14, pp. 5601–5608, 2010, doi: 10.1016/j.biortech.2010.02.008.
- [55] F. Yao, Q. Wu, Y. Lei, W. Guo, and Y. Xu, “Thermal decomposition kinetics of natural fibers: Activation energy with dynamic thermogravimetric analysis,” *Polym. Degrad. Stab.*, vol. 93, no. 1, pp. 90–98, 2008, doi: 10.1016/j.polymdegradstab.2007.10.012.
- [56] G. Mishra and T. Bhaskar, “Non isothermal model free kinetics for pyrolysis of rice straw,” *Bioresour. Technol.*, vol. 169, pp. 614–621, 2014, doi: 10.1016/j.biortech.2014.07.045.
- [57] J. D. Badía Valiente, “Strategies and analytical procedures for a sustainable plastic waste management. An application to poly (ethylene terephthalate) and polylactide in the packaging sector.,” Editorial Universitat Politècnica de València, Valencia (Spain), 2011.
- [58] IEA Bioenergy. Emerging Gasification Technologies for Waste & Biomass. 2020.
- [59] James AK, Thring RW, Helle S, Ghuman HS. Ash management review-applications of biomass bottom ash. *Energies* 2012;5:3856–73. doi:10.3390/en5103856.
- [60] Salinas CT, Pu Y, Lou C, dos Santos DB. Experiments for combustion temperature measurements in a sugarcane bagasse large-scale boiler furnace. *Appl Therm Eng* 2020;175:115433. doi:10.1016/j.applthermaleng.2020.115433.
- [61] Kleinhans U, Wieland C, Frandsen FJ, Spliethoff H. Ash formation and deposition in coal and biomass fired combustion systems: Progress and challenges in the field of ash particle sticking and rebound behavior. *Prog Energy Combust Sci* 2018;68:65–168. doi:10.1016/j.pecs.2018.02.001.



UNIVERSITAT
POLITÈCNICA
DE VALÈNCIA



ESCOLA TÈCNICA
SUPERIOR ENGINYERIA
INDUSTRIAL VALÈNCIA

ECONOMIC STUDY

In this section are presented the approximate budget of all the costs associated with the realization of this project. Both labor and maintenance costs are taken into account as well as amortization of equipment and tools, all materials (tools of laboratory) and additional expenses necessary to carry out the project.

The evaluation is divided in:

1. Labour cost
2. Equipment and Instrumentation cost
3. Fungible materials cost
4. Other costs
5. Final cost

1. LABOUR COST

This section includes the expenses of the personnel dedicated to the study. These costs will be evaluated by fraction of time, applying the price in €/h. The people who worked on the project mainly were the student and the co-directors responsible for the supervision of the project (responsible). The budget referring to the hand of work is observed in **Table 5.1**.

Table 5.1. Summary of the costs due to labour.

REF	Description	Price [€/h]	Hours [h]	Amount [€]
O1	<i>Titulado superior (student)</i>	20	700	14000
O2	<i>Doctor Contratado (tutor)</i>	30	150	4500
O3	<i>Catedratico de Universidad (supervisor)</i>	51.4	50	2570
			TOTAL	21070 €

The table shows the budget referring to labour where the hours have been calculated from the almost five months in which the project has been developed (about 100 days), removing the holidays and considering 5 days per week and 7 hours per day. The hours of the tutor were considered as 1.5 hours per day while those of the supervisor have been calculated as 2.5 hours per week.

2. EQUIPMENT AND INSTRUMENTATION COST

This section details the amortization cost of the equipment and tools that will not be acquired expressly for the study, since the Research Group in Functionalization, Degradation and Recycling of Polymer Materials from the Institute of Technological of Materials (ITM) of the Polytechnic University of Valencia (UPV), already has them (**Table 5.2**). In this way, it is considered that an investigation team is amortized. In a period of 10 years, the acquisition of tools and tools is amortized in 12 years and the acquisition of computer applications and the personal computer in 6 years. Starting from this base, the price for the present study is detailed.

Table 5.2. Summary of the costs of amortization of the equipment and instrumentation.

REF	Description	Acquisition price [€]	Amortization price [€/year]	years	Amount [€]
E1	<i>Precision balance</i>	2000	200	0.45	90
E2	<i>Thermo-gravimetric analyser Mettler Toledo TGA 851</i>	70000	7000	0.45	3150
E3	<i>University computer</i>	1000	100	0.45	45
E4	<i>Vacuum oven Heraeus Vacuthem</i>	4200	420	0.45	189
E5	<i>Muffle Furnace Heraeus</i>	6000	600	0.45	270
E6	<i>CHNS-O Thermo Flash 2000 elemental analyser</i>	5000	500	0.45	225
TOTAL					3969 €

Where the time (years) have been calculated considering 100 days for the work and dividing it for 220 productive days in one year.

3. FUNGIBLE MATERIAL COST

This group includes all non-depreciable materials that was fully consumed for the realization of this work, therefore, the price applied is that of the value of acquisition. These costs include raw materials and reagents (Table 5.3) and laboratory materials (Table 5.4).

Table 5.3. Summary of the costs of raw materials and reagents.

REF	Unit	Description	Acquisition price [€]	Quantity	Amount [€]
R1	<i>L</i>	<i>Distilled water</i>	0.20	60	12
R2	<i>tank</i>	<i>Oxygen</i>	75	0.25	18.75
R3	<i>L</i>	<i>Acetone</i>	40	0.01	0.4
R4	<i>kit</i>	<i>ORISC kit</i>	22.9	1	22.9
R5	<i>kit</i>	<i>WHEAT kit</i>	18.9	1	18.9
R6	<i>kg</i>	<i>Pilsener malt</i>	1.95	1	1.95
R7	<i>kg</i>	<i>Trigo malt</i>	1.95	1	1.95
R8	<i>kg</i>	<i>Pale Ale malt</i>	1.95	1	1.95
R9	<i>kg</i>	<i>Carafa malt</i>	1.95	1	1.95
R10	<i>kg</i>	<i>Crystal malt</i>	1.95	1	1.95
R11	<i>kg</i>	<i>Aroma malt</i>	1.95	1	1.95
TOTAL					84.65 €

Table 5.4. Summary of the costs of laboratory materials.

REF	Unit	Description	Acquisition price [€]	Quantity	Amount [€]
M1	<i>unit</i>	<i>Perforated alumina crucibles – capacity=70 µL</i>	10	30	300
M2	<i>unit</i>	<i>Tweezers</i>	7	1	7
M3	<i>unit</i>	<i>Alumina pans</i>	220	1	220
TOTAL					527 €

So, summing the costs of raw materials, reagents and laboratory materials, the total cost in this section is **611.65 €**.

4. OTHER COSTS

In this section, all the expenses related to office supplies, licenses of software and the consumption of electricity and water that has been needed for the work were considered. The summary is shown in **Table 5.5**.

Table 5.5. Summary of additional costs.

Description	Amount [€]
Laboratory materials	100
STARe Mettler Toledo license	1500
Electricity and water consumption	100
TOTAL	1700 €

5. FINAL COSTS

The final cost of the work is considered as the sum of all the previous sections and adding the value-added tax (VAT), as illustrated in **Table 5.6**.

Table 5.6. Summary of all costs.

Description	Amount [€]
Labour cost	21070
Equipment and Instrumentation cost	3969
Fungible material cost	611.65
Other costs	1700
PARTIAL TOTAL	27350.65 €
VAT 21%	5743.64 €
TOTAL	33094.29 €

The total budget for the realization of this Final Master-Degree Project amounts to THIRTY-THREE THOUSAND NINETY-FOUR EUROS WITH TWENTY-NINE CENTS, € 33094.29.

In the present work, labor was not to be paid out, for this reason, in the next table (**Table 5.7.**) is illustrated the actual budget for the project.

Table 5.7. Summary of all real costs.

Description	Amount [€]
Equipment and Instrumentation cost	3969
Fungible material cost	611.65
Other costs	1700
PARTIAL TOTAL	6280.65 €
VAT 21%	1318.94 €
TOTAL	7599.59 €



So, in the actual project the total budget for the realization of this Final Master-Degree Project decreases to SEVEN THOUSAND FIVE HUNDRED NINTY-NINE EUROS WITH FIFTY-NINE CENTS, € **7599.59**.